Energy, Mines and Resources Canada
Earth Physics Branch
1 Observatory Crescent
Ottawa Canada
K1A 0Y3

Énergie, Mines et Ressources Canada
Direction de la physique du globe
1 Place de l'Observatoire
Ottawa Canada
K1A 0Y3

GEOMAGNETIC SERVICE OF CANADA

Magneto-Telluric Reconnaissance Survey in the Lillooet Valley British Columbia

Pham Van Ngoc

40 pp.
Price $8.00

Earth Physics Branch Open File No. 77-20(E)
Ottawa, Canada
1977

Department of Energy, Mines and Resources
Canada

MAGNETO-TELLURIC RECONNAISSANCE SURVEY IN THE LILLOOET VALLEY, BRITISH COLUMBIA

by

PHAM VAN NGOC

MAGNETO-TELLURIC (M.T.) RECONNAISSANCE SURVEY IN THE LILLOOET VALLEY, BRITISH COLUMBIA

CONTENTS

ABSTRACT

A reconnaissance M.T. survey has been done in the Lillooet Valley (British Columbia) between Pemberton Meadows and Meager Mountain. A total number of 40 M.T. profiling stations were distributed along four profiles. Five M.T. sounding stations were recorded at three different sites along the valley.

Two layers were located in the overburden by the M.T. results. A first layer with a resistivity of 1000-3000 Ωm and a thickness of 45-65 m corresponds to gravel. The second layer with a very low resistivity of 2-5 Ωm and a thickness of 4-5 m corresponds to volcanic ash.

The basement has the special characteristic of being successively anisotropic and isotropic from one site to the next; the anisotropy principal directions are roughly N.S. and E.W. In the E.W. direction the basement resistivity is quite uniform, in the order of 20,000 Ωm, while on the N.S. direction this resistivity could go lower than 100 Ωm. This resistivity low might be due to wide zones of subvertical fractures caused by the recent opening of a N.S. rift system. This system could be responsible for the Garibaldi linear volcanic belt. Lastly, the results show that the earth's crust in this area is relatively shallow; its thickness is on the order of 20 km and it rests on an abnormally conductive layer with a resistivity of 10 Ωm which confirms the existence of an intensive heat source at the crust base.

MAGNETO-TELLURIC (M.T.) RECONNAISSANCE SURVEY IN THE LILLOOET VALLEY, BRITISH COLUMBIA

1 - INTRODUCTION

As stipulated in a recent agreement between the Department of Energy, Mines and Resources, Canada and the Mineral Exploration Research Institute, a reconnaissance magneto-telluric survey was carried out in the Lillooet valley (B.C.)between Pemberton Meadows and Meager Mountain. The survey was done during July 1976 with the purpose of obtaining information on the rock resistivity distribution both at surface and at depth relative to any hot water sources and geothermal flux. Meager Mountain is indeed one of the 32 quaternary volcanoes of the Garibaldi volcanic belt aligned approximately in a N.S. direction.

The original program consisted of four primary magneto-telluric sounding stations and 40 secondary profiling stations distributed along two 2 km profiles running across the Lillooet valley.

Let us recall that magneto-telluric sounding (M.T.S.) measures variations of the apparent resistivity ρ_a as a function of the period T (or $\sqrt{T}$) in order to get quantitative data on the depth and resistivity of the different underground formations. Magneto-telluric profiling (M.T.P.) detects the lateral variations of the apparent resistivity ρ_a measured at selected discrete periods (or frequencies); these variations are presented as profile or semi-quantitative cross-section (pseudo-section).

2 - GEOGRAPHICAL LOCATION

In the field we were guided by Dr. L.Law of the Department of Energy, Mines and Resources, Canada who helped with the selection of the station sites; however the original program has been slightly modified due to accessibility problems encountered during profiles execution. As a result, instead of two profiles with a nominal length of 2 km we have done four shorter profiles at the three different sites along the Lillooet valley. In addition to these, five soundings (instead of four) were done at these three sites. Figure 1 shows the geographical location of the sites on a 1 : 250,000 scale map and Figure 2 shows the same sites on a larger scale aerial photograph. Detail sketches showing the location of the four profiles are presented in Figures 3, 4 and 5. Table 1 lists the distribution of the magneto-telluric profiling (M.T.P.) stations and the magneto-telluric sounding (M.T.S.) stations.

TABLE I

Profiles	M.T.P. Stations	M.T.S. Stations
P.I	1 to 5	S.1
P.II	1 to 9	S.2
P.III	1 to 16	S.3 and S.4
P.IV	1 to 10	S.5

This adds up to a total of 40 M.T.P. stations and 5 M.T.S.stations.

3 - INSTRUMENTATION AND DATA ACQUISITION

3-1 Magneto-telluric profiling (M.T.P.)

The instrument used for M.T. profiling, the "TELMAG 2" (TELluric-MAGneto-telluric) has been designed and built at the Applied Geophysic Laboratory of Ecole Polytechnique de Montreal. This unit could be used for magneto-telluric profiling as well as telluric-telluric profiling (Pham Van Ngoc 1975, 1976). It is made up essentially of two identical "filter-amplifiers". Each of these is housed in a 37x36x15 cm fiberglass case and weighs about 8 kg (see figures 6 and 7). Figure 8 is a block diagram of the filter-amplifier. The 60 and 180 hz notch filter is used to eliminate industrial noise coming from power lines. There are four very selective pass-band filters working in parallel so that the signals at four different frequencies are measured simultaneously in four distinct channels. Moreover each channel can be tuned to three different frequencies so that a total of 12 frequencies can be analysed; these frequencies are : 1, 3, 5, 8, 21, 34, 100, 250, 400, 700, 1200 and 2000 hz. Because of this feature the "TELMAG 2", if desired, could also be used to really produce a "M.T. mini-sounding" in this frequency span. The pseudo-sinusoidal signals are rectified at the output of the selective filters and integrated; the average voltage is displayed on a liquid crystal display digital voltmeter so that the readings are easily made even in bright sunlight. The signal levels are controlled by analog meters, any saturation is detected and displayed by a pilot light and the integration time is automatically controlled by four clock signals one for each channel.

During magneto-telluric profiling one of the "filter-amplifier" of the "TELMAG 2" is connected to the telluric sensor while the other one is connected to the magnetic sensor. The telluric sensor is made of two stainless steel electrodes driven directly into the ground. The magnetic sensor (CM-15) is an inductive type with a ferrite core and flux feedback giving a flat response in a wide span of frequencies : about 50 mV/Y between 5 and 500 hz. The profiling data does not need any particular processing. For each station at every given frequency the procedure is simply to take an average of 3 to 4 readings of the values of the telluric and magnetic field and then to apply Cagniard's formula to get the apparent resistivity at that frequency (or period) :

$$\rho_{ax} = 0.2\ T \left| \frac{E_x}{H_y} \right|^2$$

ρ_{ax} = apparent resistivity in Ωm

T = period in seconds

E_x = component of the telluric field in the Ox direction in mV/km

H_y = component of the magnetic field in the Oy direction (perpendicular to Ox) in gamma.

By convention the value of apparent resistivity obtained according to this procedure is assigned to the direction of the telluric line.

3-2 Magneto-telluric sounding (M.T.S.)

The magneto-telluric sounding system has been essentially designed to be entirely mobile either by a small truck or, in remote

access areas, by helicopter; it uses a Tandberg TIR 115 - 4 channel analog tape recorder with a signal to noise ratio of 48 dB. Figure 9 shows the block diagram of the measuring system. Each channel is made of a wide band filter ITHACO 4210 with a very high input impedance, a very low noise preamplifier PAR 113 and a 60+180 hz notch filter together with an amplifier connected to the Tandberg recorder. In the case of M.T. sounding, because of the very wide frequency range of the signals to be analysed, there are several types of tellurics and magnetics sensors :

Frequency range	Telluric sensors	Magnetics sensors Flat response
Frequency > 1hz	Steel electrodes	CM.15 (5-500hz)≃50mV/γ
Frequency < 1hz	Non-polarisable electrodes ($CuSO_4$)	CM.9R (0.1-50hz)≃50mV/γ CM.9L (0.005-1hz)≃10mV/γ

As the CM.15, the CM.9R and CM.9L are of the inductive type with flux feedback but with a mu-metal core. At each station, a simultaneous recording is made of two horizontal telluric components E_x and E_y and two horizontal magnetic components H_x and H_y along two perpendicular directions Ox et Oy; this is done so that later the principal directions and apparent resistivities will be obtained through tensor processing. A simultaneous recording of the vertical magnetic component is also made with either E_x and E_y or H_x and H_y to complete the above information in the case of lateral resistivity discontinuities.

The analog magnetic recordings are briefly analysed in the field as a recording quality check. They are later digitized in the laboratory with anti-aliasing filters and sampling rates appropriate for the frequency ranges processed.

4 - MTS DATA PROCESSING

Let us recall that the tensor processing of MTS data is done in order to get tensor impedances Z_{ij} along the principal directions in the case of an electrically anisotropic ground. Of course in the tabular case, the tensor impedances degenerate into scalar Cagniard impedances which are independent of the measuring axis directions. In the general case, the four horizontal magneto-telluric components are related by the following equations :

$$E_x = Z_{11}H_x + Z_{12}H_y$$

$$E_y = Z_{21}H_x + Z_{22}H_y$$

The four terms of the Z_{ij} tensor are evaluated by the least square method which has the advantage of minimising the noise particularly on the telluric records.

If the ground has a two dimensional electric anisotropy, the angle θ_0 between the anisotropy axes and the measuring axes is given by :

$$t_g\ 4\ \theta_0 = \frac{(Z_{11}-Z_{22})(Z_{12}+Z_{21})^{*}+(Z_{11}-Z_{22})^{*}(Z_{12}+Z_{21})}{|Z_{11}-Z_{22}|^2-|Z_{12}+Z_{21}|^2}$$

However in order to get a better view of the two-dimensional character of the electrical anisotropy of the ground, an examination is made of

the variation of the 4 terms of the Z_{ij} tensor for each period as the measuring axes are rotated by 5^{o} increments between -90^{o} and $+90^{o}$. Figure 10 shows an example of such an analysis. The two directions θ^{o} and $\theta^{o}+90^{o}$, for which the diagonal term Z_{11} (or Z_{22}) is zero or minimum, correspond to the two principal directions of the electrical anisotropy. The corresponding values of the Z_{12} and Z_{21} terms permit the calculation of the two principal apparent resistivities $\rho_{a_{12}}$ and $\rho_{a_{21}}$. Figure 11 shows the flow chart of the MTS tensor data processing program.

5 - MAGNETO-TELLURIC PROFILING RESULTS

Forty (40) M.T.P. stations were done on the three measuring sites (see fig. 2) and distributed along 4 profiles as shown in Table I. The specific location of each station has been noted and is shown on Figures 3, 4 and 5.

As we did not have any information on the survey area's tectonics, we first made a few tests to determine the telluric line direction. We have thus observed that the telluric field is highly polarized in the E.W. direction and that in this particular direction the telluric component has a better correlation with the orthogonal magnetic component. Moreover it is also the approximate general direction of the Lillooet valley. Based on these observations we have adopted the following directions for the telluric line :

- profile P.I and P.II : 60^{o} N.E. relative to magnetic north

- profile P.III and P.IV : E.W. magnetic.

This direction change is due to the local change in the valley's direction. The tests have shown that a 50 m length of telluric line gives a good signal level.

As already stated in the introduction, the purpose of M.T.P. is to detect the lateral variations of resistivity; these can be observed by presenting the results as profiles for each frequency or as pseudo-sections giving a more complete view of the results laterally as well as in depth. However, the results constitute a genuine "M.T. mini-sounding" since the TELMAG 2 instrument can measure apparent resistivities over 12 distinct frequencies regularly distributed on a logarithmic scale between 1 and 2000 hz. As examples, 8 curves of these "mini-soundings", corresponding to 8 M.T.P. stations, have been shown on figures 12 to 19; two stations for each of the 4 profiles have been selected for these curves. On these figures the VLF apparent resistivity, as measured by the EM16R at 18.6 Khz, has also been plotted in addition to the 12 "TELMAG 2" frequencies.

The following observations are based on the examination of these curves :

- In general there is a good continuity in the apparent resistivity values; the high frequencies (2000 hz and 1200 hz) which have a very low signal to noise ratio are an exception to this statement.
- When the VLF apparent resistivity is included all the sounding curves have the shape of a 4 layer curve with an extremely high resistivity contrast.

- All the curves from the 40 M.T.P. stations have very similar shapes especially among stations of the same profile.

The 4 M.T.P. profiles are shown completely as pseudo-sections in Figures 20 to 23. The very uniform character of the superficial cover on the survey area is confirmed by these figures because the ρ_{ax} iso-resistivity lines are practically horizontal in the high frequencies. The apparent resistivity rises very rapidly toward the low frequencies, from 30-50 Ωm around 2000 hz to a maximum of 5000-10000 Ωm between 3 and 8 hz. Thus the profiling results seem to indicate that the basement has well been reached and even the base of the earth's crust. Toward the low frequencies a few irregularities in the apparent resistivities are spotted by the pseudo-sections. However these irregularities are entirely local with an extent of approximately 50 to 100 m and could only come from the irregularities on the superficial cover especially when the latter includes a very conductive layer as is presently the case. Therefore we could conclude that within a radius of a few kilometers the M.T.P. profiles across the Lillooet valley have not shown any large resistivity variations at the basement level.

6 - MAGNETO-TELLURIC SOUNDING RESULTS

The M.T. soundings as done in this survey, are of the "crossed sounding" type : these consist of a simultaneous recording, along two perpendicular directions, of two telluric components and two

telluric components and two horizontal magnetic components. The two directions used were the following :

- Sounding S.1 and S.2 : 30^{o} N.W. magnetic and 60^{o} N.E. magnetic
- Sounding S.3, S.4 and S.5 : N.S. and E.W. magnetic

The telluric lines, along the two directions, have a 200 m length. The frequency band of the signals processed for the soundings is limited from 0.1 hz to 500 hz (i.e. periods of .002 to 10 sec). The high frequency limitation is based on the fact that over 500 hz the signal to noise ratio is very weak so that a wide bandwidth recording does not give good results. On the low frequency side, the M.T. profiling results show that a 10 second period is quite enough for the study of the basement electrical properties.

Generally a very good magneto-telluric correlation could be observed on the signals within the recorded frequency band especially toward the high frequencies. An example of these signals in the 1-500 hz band is shown on Figures 24 and 25. An examination of coherences (see figures 26 and 27) shows that the correlation is much better between E.W. and H than between N.S. and D. The same characteristics are observed for all the five soundings and could be explained by the fact that the telluric field is highly polarized along the E.W. direction and thus the signal to noise ratio is higher in that direction. It is also apparent, relatively to all the soundings, that the coherences are weaker for periods longer than 1 second.

The tensor processing, as already described, has been applied to all the five soundings and the results are displayed in Figures 28 to 32. These results will be commented on, in detail, below.

M.T.S. S.1 : Figure 28 shows the two apparent resistivity curves ($\rho_{a_{12}}$, $\rho_{a_{21}}$) along the two principal directions. Figure 22 shows one of the two principal directions (θ_{12}) for each sounding; the other principal direction (θ_{21}) is given by $\theta_{12} + 90^{o}$. In fact two values for θ_{12} are displayed : θ_{012} is the value given by the formula yielding tg 4 θ_0 and $\theta_{min_{12}}$ is the value given by the method shown in Figure 10. The θ_{min} values are more homogeneous so that the $\rho_{a_{12}}$ and $\rho_{a_{21}}$ apparent resistivities plotted on Figure 28 are obtained by using this processing method.

The $\rho_{a_{12}}$ and $\rho_{a_{21}}$ curves show a very high electric anisotropy for the basement under the station S.1 : $\rho_{a_{21}}$ is 20 to 30 times higher than $\rho_{a_{12}}$. The principal directions of anisotropy are approximately N.S. ($\rho_{a_{12}}$) and E.W. ($\rho_{a_{21}}$). The anisotropy weakens toward the short periods (T < .005 sec) and probably also toward the long periods (T > 10 sec). The $\rho_{a_{21}}$ curve has the same shape as the "mini-sounding" curves obtained by the profiling results (see Figures 12 and 13). This is why we have performed a tentative extrapolation (toward the short periods) of the $\rho_{a_{21}}$ mean curve plotted as a dashed curve based on the results of the M.T.P. P.I. The $\rho_{a_{12}}$ curve is more complex and it is difficult to provide a satisfactory explanation considering the information thus far presented.

M.T.S. S.2 : The results of this sounding, displayed in Figure 29, are similar in every respect to those of sounding S.1. In fact these two soundings are located on the same site within 500 meters of each other.

M.T.S. S.3 and S.4 : These two soundings are also located on the same site and their results are very similar (see Figures 30 and 31). The most striking feature relatively to the previous results is that the basement shows an isotropic response. Therefore there are no principal directions. The shape of the apparent resistivity curve is once again similar to the "mini-sounding" curves of the M.T.P. P.III (see Figures 16 and 17).

M.T.S. S.5 : As was the case with soundings S.1 and S.2, the basement response is again anisotropic. The comments applicable to S.1 and S.2 are also applicable to S.5 with the following exceptions : the S.5 anisotropy is weaker ($\rho_{a_{21}}$ is only 10 times higher than $\rho_{a_{12}}$) and the θ_{12} principal direction shows a greater dispersion particularly toward the periods longer than 1 sec.

7 - EXAMINATION OF THE MAGNETIC VERTICAL COMPONENT TRANSFER FUNCTION (H_z) AND INTERPRETATION OF THE PRINCIPAL DIRECTIONS

The anisotropic character of the tensor apparent resistivities for soundings S.1, S.2 and S.5 could be explained :

1) Either by the existence of a major tectonic feature in the basement (a fault or a fracture zone) elongated along one of the two principal directions,

2) Or by a two-dimensional electric anisotropy (macro anisotropy) in the basement.

In the first case we should observe a vertical magnetic field H_z directly related to the longitudinal component of the telluric field (i.e. parallel to the structure) or to the transverse component of the magnetic field. Moreover, it is well known, by our theoretical and experimental results (Pham Van Ngoc and Boyer, D., 1974) that the transverse apparent resistivity is highly distorted by the superficial structure heterogeneity even for very long periods. Figure 34 is an example of a theoretical response showing how the two soundings diverge depending on the type of polarization : E or H. According to these results, if the observed anisotropy at soundings S.1, S.2 and S.5 was caused by a two-dimensional heterogeneity, the longitudinal direction of the latter would be parallel to the principal direction θ_{21} i.e. approximately E.W.

The determination of a two-dimensional heterogeneity's longitudinal direction could be done by an examination of the vertical magnetic component H_z according to the following complex relation :

$$H_z = AX + BY$$

X and Y are respectively either the two telluric components E_x and E_y, or the two magnetic components H_x and H_y, while A and B are complex coefficients termed the "transfer functions".

While turning the Ox and Oy axis, A and B follow an ellipse in the complex plane as a function of the rotation angle β. Knowing that $A(\beta) = B(\beta+90^{o})$, the angle $\beta_0 \pm 90^{o}$ corresponding to the ellipse's two axes is given by the formula :

$$\text{tg } 2\,\beta_0 = \frac{AB^* + BA^*}{AA^* - BB^*}$$

Moreover, by the determination of the ellipticity r :

$$r = \frac{B(\beta_0)}{A(\beta_0)}$$

The ellipse's orientation is completely defined. For the case where $X = E_x$ and $Y = E_y$ the angle β_0, corresponding to the major axis of the ellipse, represents the longitudinal direction. In the case where $X = H_x$ and $Y = H_y$ it is the angle β_0 corresponding to the minor axis that represents the longitudinal direction.

This type of processing has been applied to two soundings S.1 and S.5, using the following relation :

$$H_z = AH_x + BH_y$$

The A and B coefficients are evaluated by a least squares method similar to the one used for the evaluation of the tensor impedances Z_{ij}. Figure 35 shows the longitudinal direction β_0 as a function of the period T for the soundings S.1 and S.5. One can see that there is no apparent direction for S.5. Also an examination of the coherences between H_z and H_x and also between H_z and H_y shows that these coherences are always very low, less than 0.5. With respect to station S.1, there seems to be a given direction only for the periods shorter than 0.04 sec but the β_0 angle $\simeq 35^{o}$ N.W. Mag. does not correspond to any of the principal directions θ_{12} and θ_{21} already found.

The second hypothesis is now considered; according to this hypothesis, the anisotropy in the apparent resistivity is caused by an electric macro anisotropy within the basement and probably in the whole thickness of the earth's crust. Let us take, as an example, the case of a succession of vertical layers of constant thickness equal to 100 m but with resistivities alternatively equal to 20000 Ωm and 50 Ωm (see the next included figure).

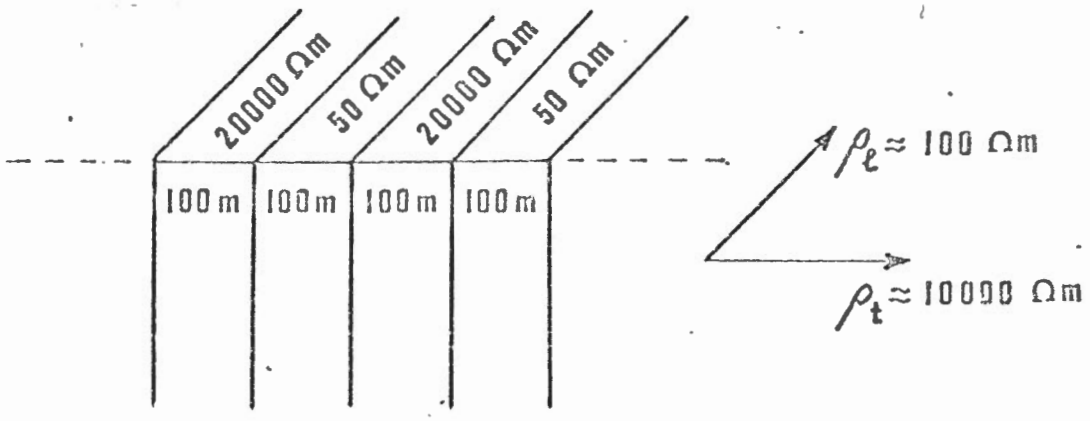

Such a succession is a typical case of macro anisotropy. Its mean transverse resistivity (perpendicular to the layers) is easily calculated as $\rho_t \approx 10000$ Ωm while its mean longitudinal resistivity (parallel to the layers) is $\rho_\ell \approx 100$ Ωm. This, on a very coarse scale, corresponds to the anisotropy in the apparent resistivities observed at the S.1 sounding. We still have to find a geological justification for this macro anisotropy.

First let us note that the principal direction of the longitudinal anisotropy θ_{12} as found at the three stations S.1, S.2 and S.5 is roughly 15° N.W. Mag. which is quite near the geographic N.S. direction. However, at first glance, it is difficult to justify

such a direction since the main tectonic directions in the Canadian Cordillera are oriented N.W. This is the case, for example, of the geanticline coastal range in which the survey area is located.

The existence of a N.S. structural direction has been proven by J.G. Souther (1970) who has noted, in particular, that the numerous recent quaternary volcanoes that belong to the Garibaldi volcanic belt are aligned along a N.S. direction (see Figure 36). While we will not present here all the arguments worked out by Souther we will quote his statement following the synthesis of the various pertaining geological and geophysical results : "In this context, it is reasonable to speculate that the linear belts of quaternary volcanoes and associated grabens may be the first expression of an opening rift system through Central British Columbia" (Souther, 1970, p. 567). According to this hypothesis, the Lillooet valley area would be under the influence of pressures caused by an E.W. expansion of the opening rift system as shown with arrows on Figure 36. The existence of an electric anisotropy as evidenced by soundings S.1, S.2 and S.5, seems to corroborate this hypothesis. In addition to the coincidence between the N.S. anisotropy direction and the Garibaldi volcanic belt direction, the numerous normal faults typical of a rift system could be the cause of the succession of numerous subvertical conductive zones within an otherwise very resistive basement.

8 - QUANTITATIVE INTERPRETATION OF M.T. SOUNDINGS

The M.T.S. curves for anisotropic structures can be interpreted as tabular and isotropic structures; it should be clear however that the basement resistivities will be different along the two principal directions. We made the choice of interpreting the transverse apparent resistivity curves $\rho_{a_{21}}$ for the soundings S.1, S.2 and S.5; there was no choice to be made for soundings S.3 and S.4 as they are isotropic. It should be noted, with respect to the latter, that considering their similarity, the same mean curve was adopted for both of them.

Figures 37 to 40 show the results obtained by the interpretation giving the resistivity RØ in Ωm and the thickness H in km for the respective layers. We could thus observe that all the soundings correspond to the following four layer geoelectric section :

45-65 m	1000 - 3000 Ωm	gravel
4-5 m	2.5 - 5.5 Ωm	clay or volcanic ash
18-21 km	20000 Ωm	granitic basement earth's crust
	10 Ωm	upper mantle

The lack of data toward the very high frequencies (from 2000 to 10000 hz) does not permit a better interpretation of the cover.

However its conductance could be evaluated with a good precision by using the asymptotic values of the rising part of the sounding curves. By this method we get :

Stations	S.1	S.2	S.3 and S.4	S.5
Conductance in mhos	1.9	2.4	1.1	2.0

A better knowledge of the superficial cover resistivities will lead to a better evaluation of its thickness from the values of conductance.

The basement on the other hand has a very high resistivity of the order of 20000 Ωm. Its thickness, which probably corresponds to the thickness of the earth's crust, is evaluated with good precision. The direct evaluation of the depth of the basement's bottom by the asymptotic values of the falling part of the sounding curves gives :

Stations	S.1	S.2	S.3 and S.4	S.5
Depth in km	20.5	21.5	17.6	19.1

In every case, these results confirm those obtained by Caner et al. (1969) and Caner (1970), but in a much more precise fashion : the earth's crust in the coastal area of British Columbia is relatively thin, its thickness is of the order of 20 km in the Lillooet valley, and the underlying layer has a very low resistivity, on the order of

10 Ωm. Caner et al. (1969), in their interpretation, have used two of the three M.T. soundings done in the western area, Penticton and Grand Forks; they found a slightly lower thickness for the earth's crust on the order of 10-15 km (Caner, 1970). However, as the shortest period used was 30 sec a better precision in the interpretation of the earth's crust was not possible. The 1000 Ωm resistivity and the 10-15 km thickness for the earth's crust are slightly underestimated relatively to our results. However the order of magnitude given by Caner et al. is remarkable considering their data dispersion. Concerning the very conductive layer at the base of the earth's crust, even if our data does not have information at periods long enough to give a better evaluation of its resistivity, we can nevertheless presume that its resistivity is on the order of 10 Ωm. This assumption is based on the high value of the falling slope of the $\rho_{a_{21}}$ curve and also on the low values of $\rho_{a_{12}}$ for periods larger than 1 sec. This 10 Ωm order of magnitude confirms Caner's hypothesis (1970) that this layer would show a high temperature combined with an hydratation and probably a partial melting of the base of the earth's crust.

9 - GEOTHERMAL INCIDENCE OF THE RESULTS OF THE M.T. SURVEY IN THE LILLOOET VALLEY

Considering the results obtained with this reconnaissance M.T. survey in the Lillooet valley, it appears that the initial project of making profiles across the valley is not a good strategy for a geothermal survey. Indeed, the M.T.P. results show that locally,

within a 2 km radius, there is little variation in resistivity at the basement level. On the other hand looking at the M.T.S. results, the basement presents along the valley some areas where the electrical properties are remarkably different; these areas might have an interesting incidence on the evaluation of the underground thermal potential.

Thus the strong electrical anisotropy as seen on the S.1 and S.2 soundings at site 1 is a very interesting problem to follow up. First the basement's transverse resistivity (in the E.W. direction) seems quite uniform along the valley, at about 20000 Ωm. Second the lows in the longitudinal resistivity (in the N.S. direction) which vary from site to site, could be related to recent deep fractures of the earth's crust; these fractures could be responsible for the Garibaldi linear volcanic belt and for thè possible hot water sources sought. A better interpretation of the longitudinal resistivity curves would eventually lead to the localization of conductive zones within the basement; these zones being of important geothermal interest. But more data and results are necessary for such an interpretation. We think that a systematic survey with magneto-telluric soundings along the Lillooet valley, with a M.T. sounding primary station every 2 km and several M.T. profile secondary stations, will provide a better localization of the fracture zones and thus a better understanding of the deep structure of the earth's crust with its geothermal inferences.

We will conclude by stating that this reconnaissance M.T. survey has proved the reliability of the magneto-telluric method in the geothermal exploration problems; this is the case even in structurally very complex areas, as the Lillooet valley, provided that the data acquisition strategy is correctly employed along with the proper equipment and sophisticated data processing and interpretation methods.

Montreal, November 25th, 1976

PHAM VAN NGOC

REFERENCES

CANER, B., CAMFIELD, P.A., ANDERSEN, F. et NIBLET, E.R. (1969). A Large Scale Magnetotelluric Survey in Western Canada. Can. J. Earth Sci., 6, pp. 1245-1261.

CANER, B. (1970). Electrical Conductivity Structure in Western Canada and Petrological Interpretation. J. Geomag. Geoelect., 22, pp. 113-129.

PHAM VAN NGOC et BOYER, D. (1974). Propriétés électriques des terrains profonds sous l'anomalie magnétique du Bassin Parisien. C. R. Acad. Sci., Paris, tome 279, série D, pp. 715-718. Magnetotelluric Mapping of Deep Structure in the Parisian Basin. Second Workshop on EM Induction, Ottawa, 22-28 août 1974.

PHAM VAN NGOC (1975). Théorie et pratique de la magnéto-tellurique et du profilage tellurique-tellurique. Theory and Practice of Magnetotelluric and Telluric-Telluric Profiling. Rapp. Tech. Ecole Polytechnique Montréal N° EP75-R-9.

PHAM VAN NGOC, BOYER, D. et CHOUTEAU, M. (1976). Nouvelle technique de cartographie de résistivités du sol par profilage tellurique-tellurique associé à la magnéto-tellurique. C. R. Acad. Sci., Paris, tome 282, série B, pp. 71-74.

SOUTHER, J.G. (1970). Volcanism and its Relationship to Recent Crustal Movement in the Canadian Cordillera. Can. J. Earth Sci., 7, pp. 553-568.

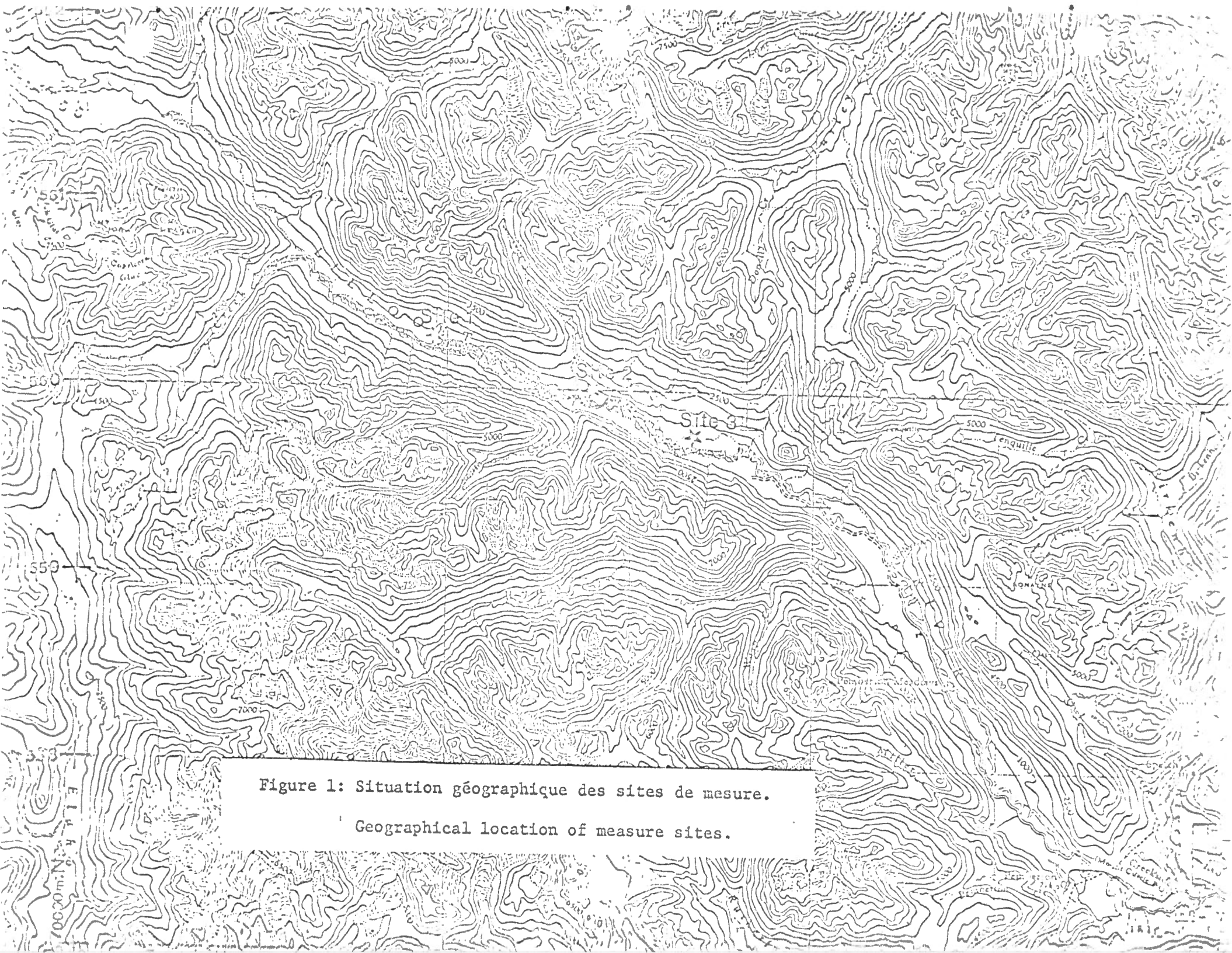

Figure 1: Situation géographique des sites de mesure.

Geographical location of measure sites.

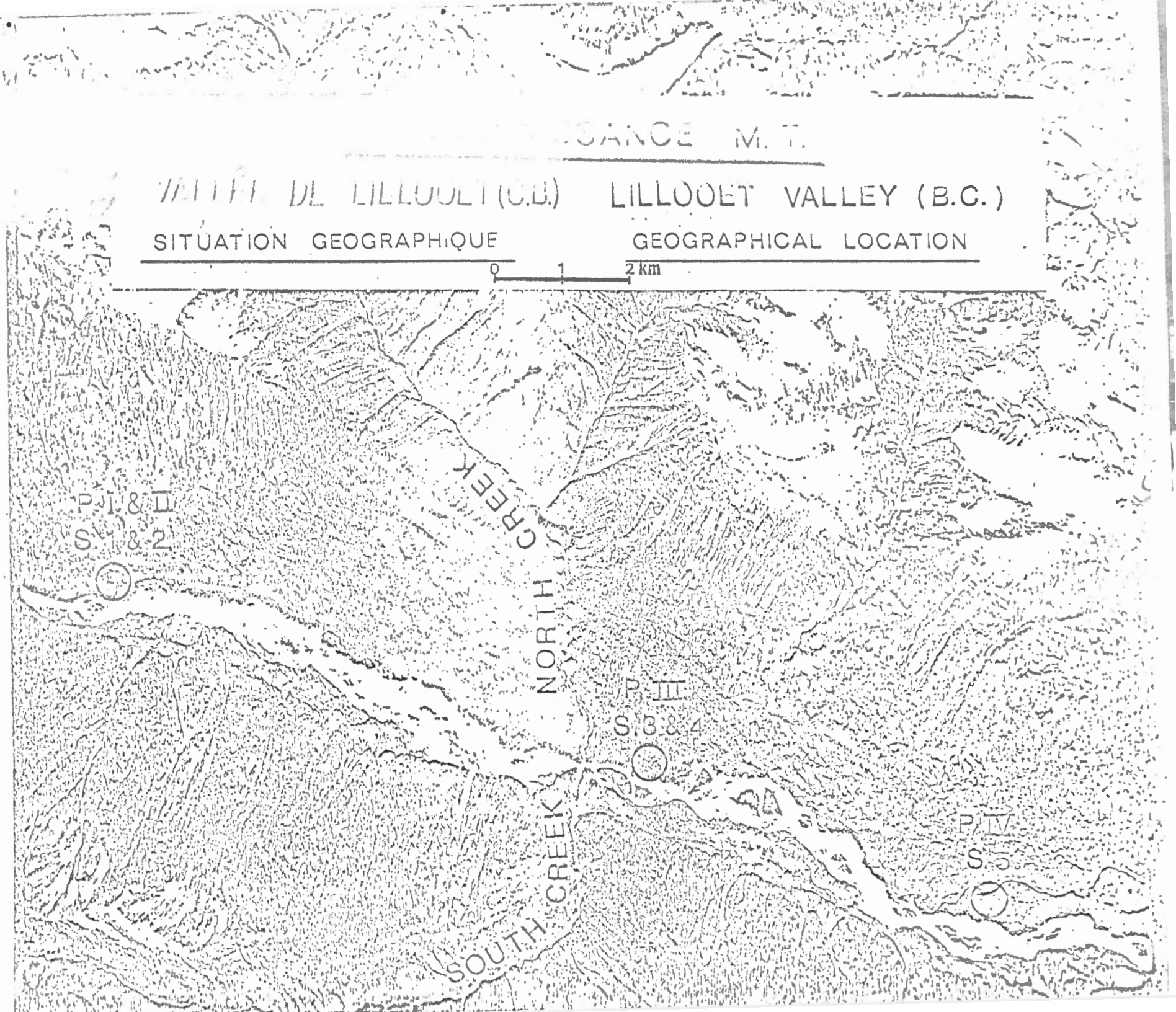
SITUATION GEOGRAPHIQUE
GEOGRAPHICAL LOCATION
LILLOOET VALLEY (B.C.)
0 1 2 km
NORTH CREEK
SOUTH CREEK
P. I & II
S. 1 & 2
P. III
S. 3 & 4
P. IV
S. 5

RECONNAISSANCE M. T.

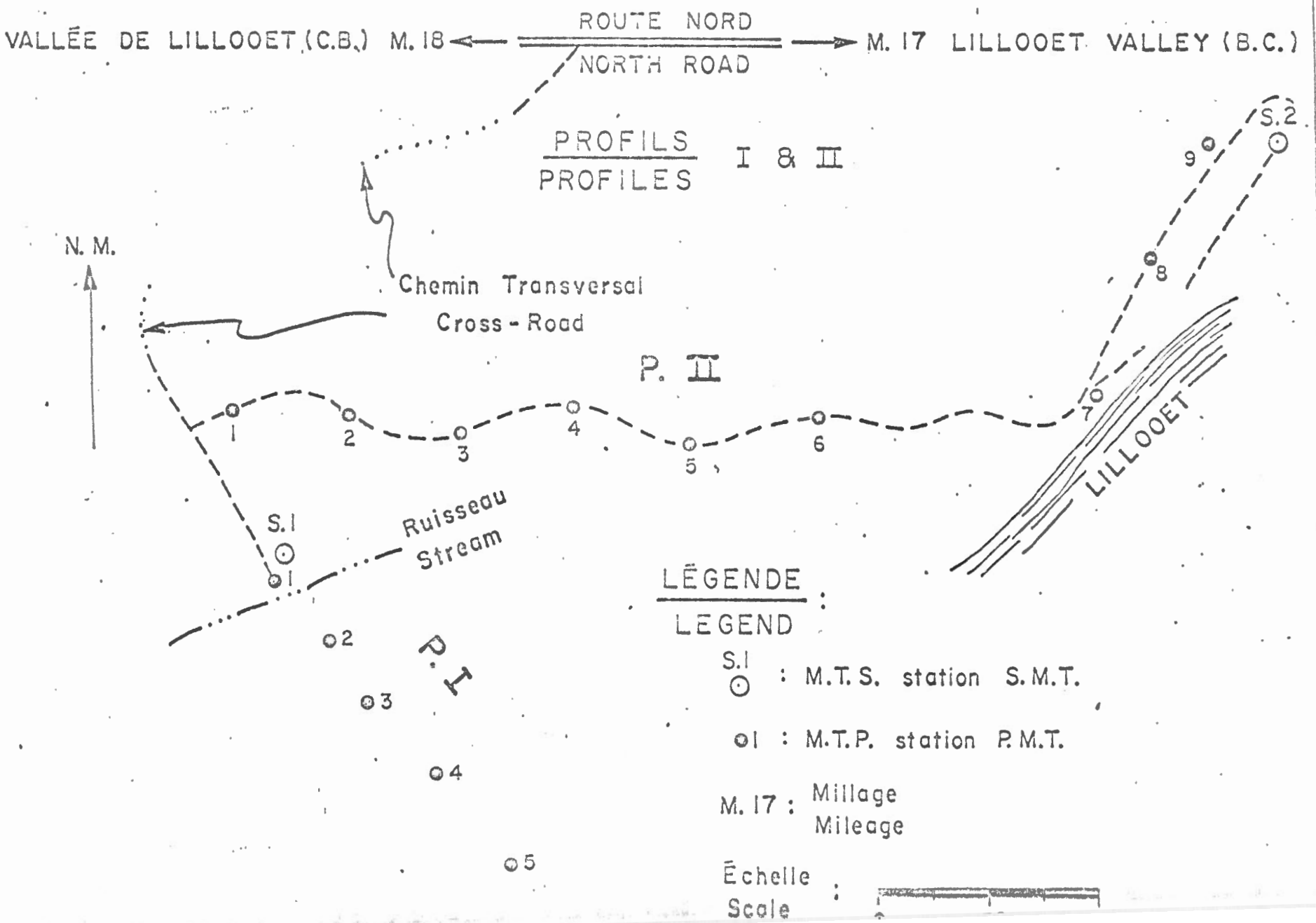

RECONNAISSANCE M. T.

VALLÉE DE LILLOOET (C.B.) — LILLOOET VALLEY (B.C.)

PROFIL / PROFILE III

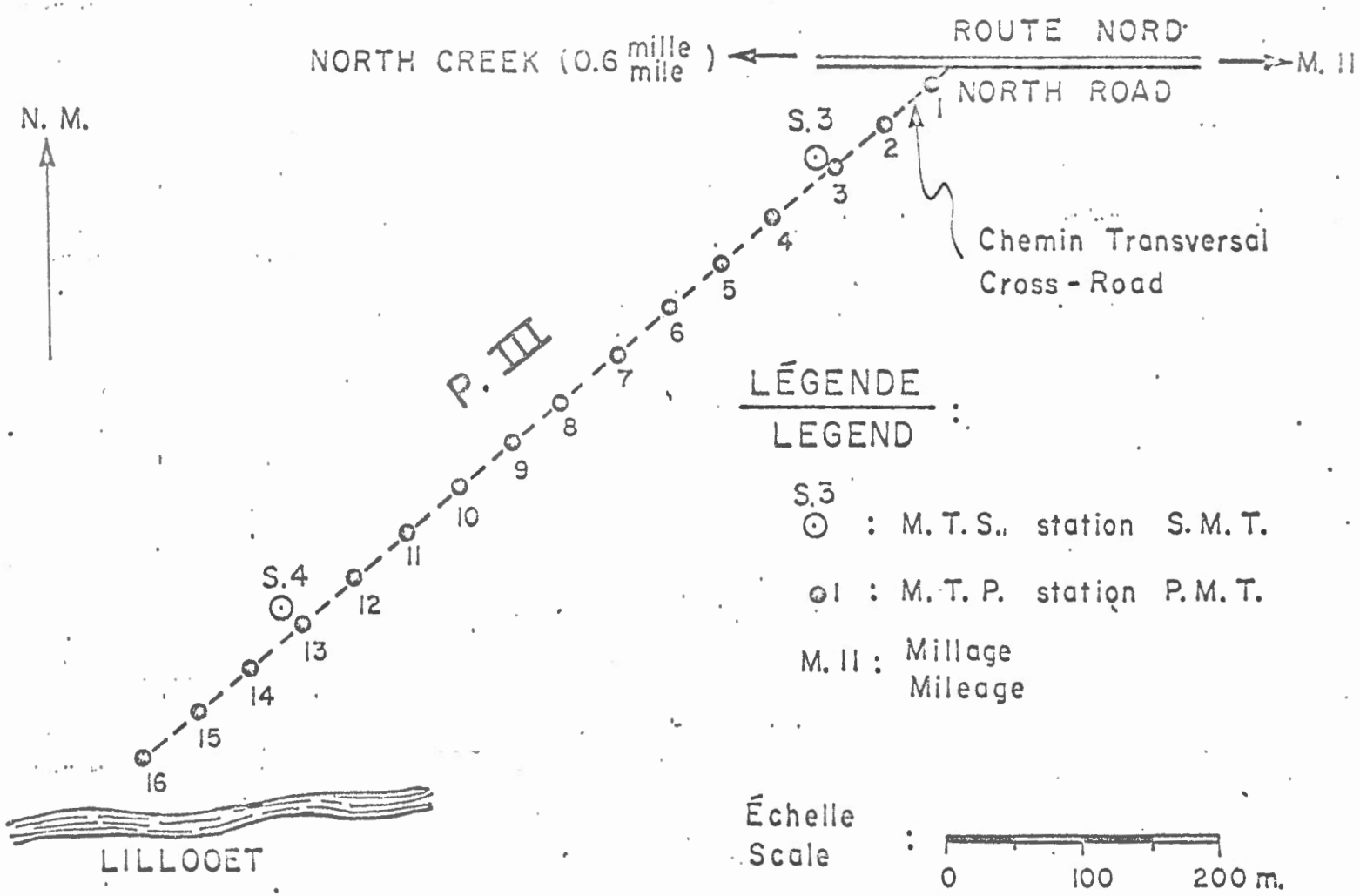

RECONNAISSANCE M. T.

VALLÉE DE LILLOOET (C.B.) — LILLOOET VALLEY (B.C.)

PROFIL / PROFILE IV

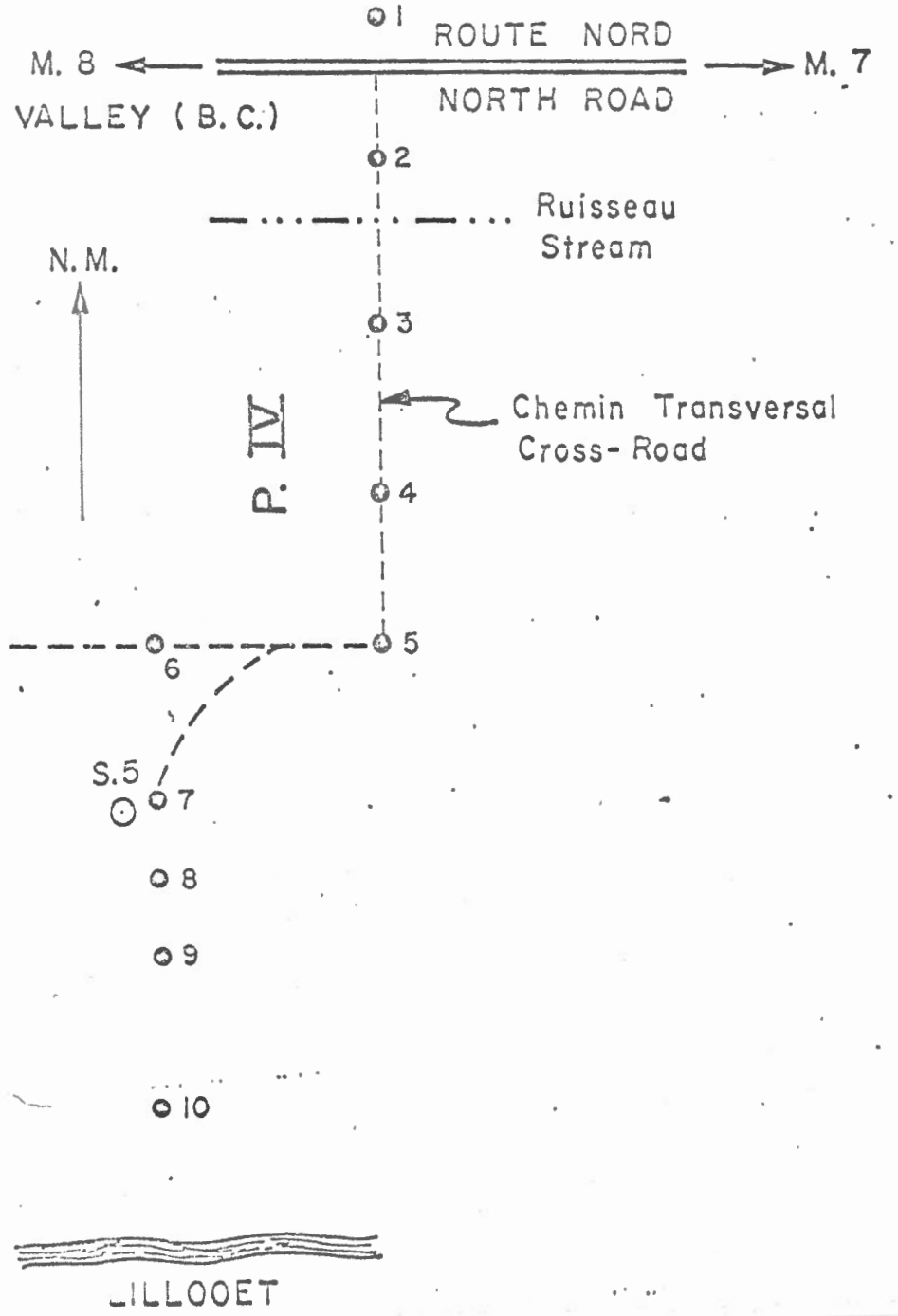

LÉGENDE / LEGEND :

S.5 ⊙ : M.T.S. station S.M.T.

o1 : M.T.P. station P.M.T.

M.7 : Millage / Mileage

Échelle / Scale : 0 — 100 — 200 m.

Figure 6: Appareil de profilage "TELMAG 2" mis en station pour une mesure magnéto-tellurique.

Equipment for profiling "TELMAG 2" located at a station for M.T. measurement.

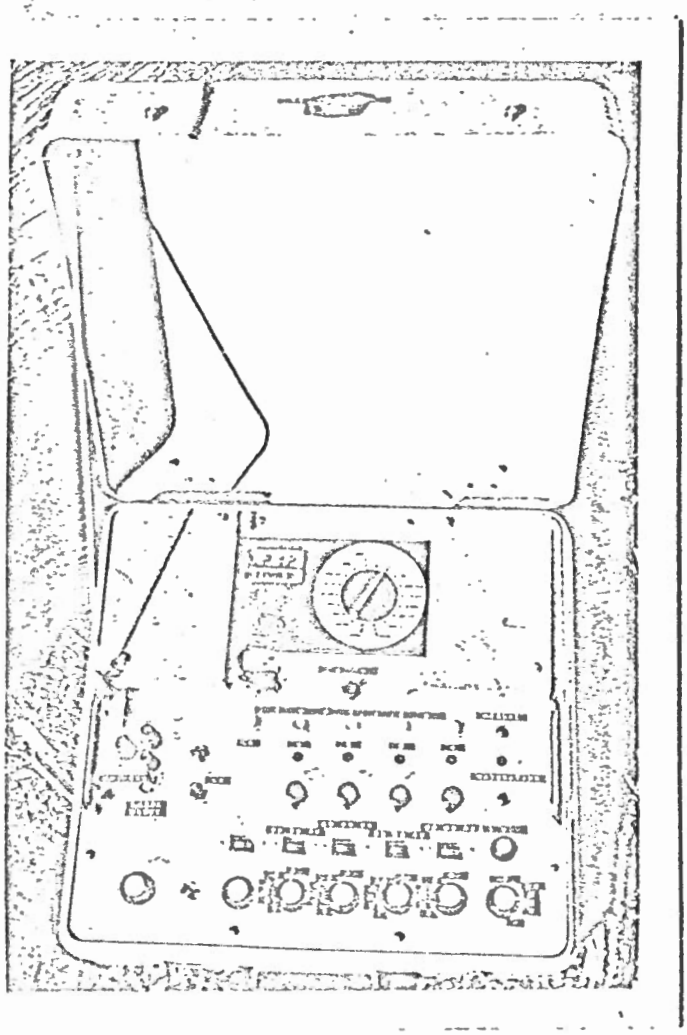

Figure 7: Panneau de contrôle de la valise "amplificateur-filtre".

Panel control of "amplifier-filter" box.

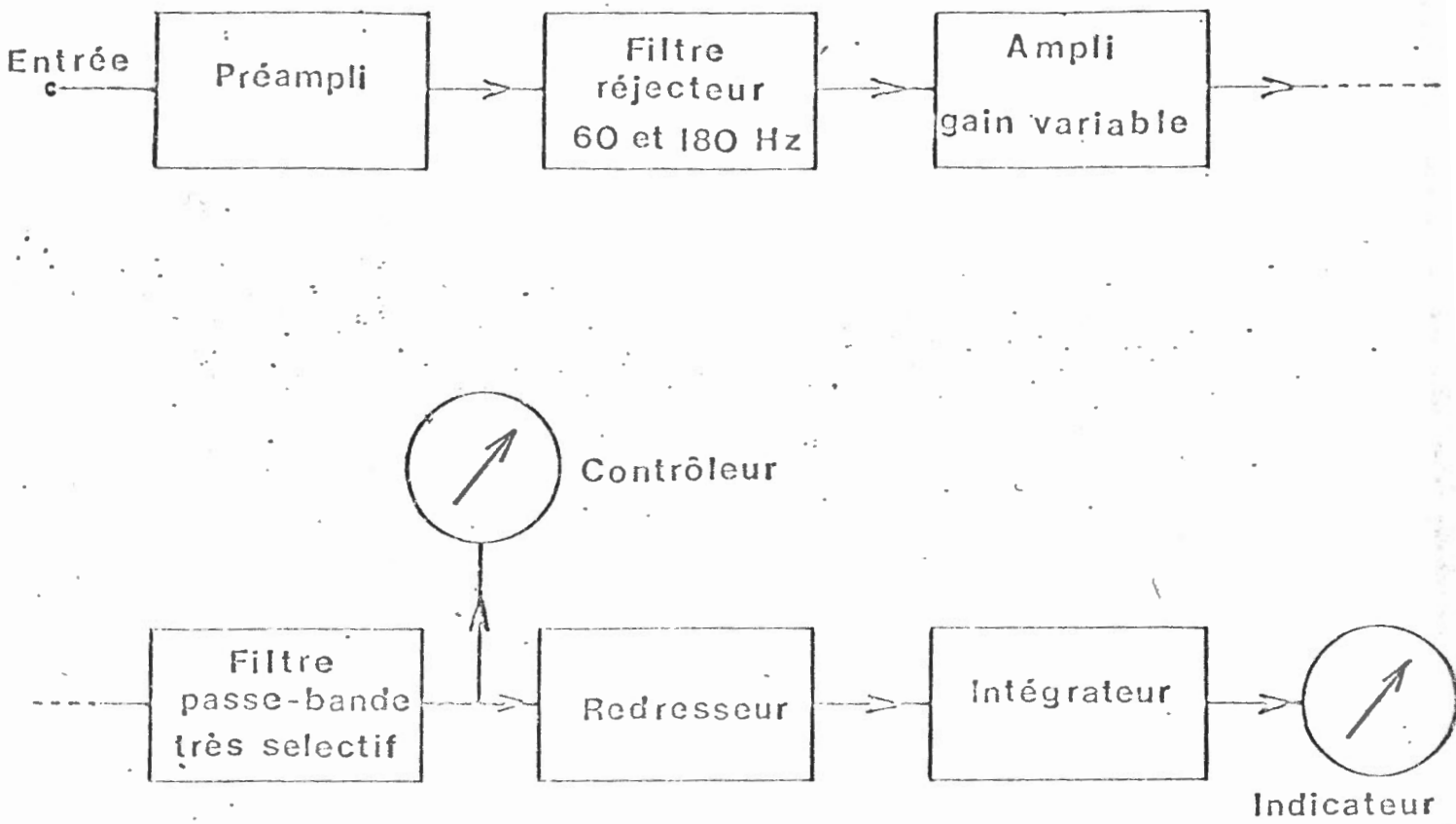

Figure 8: Schéma synoptique de l'amplificateur-filtre.

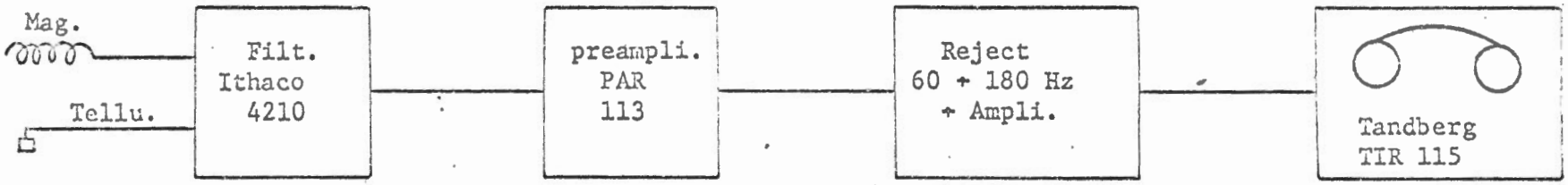

Figure 9: Schéma synoptique de la chaîne de sondage magnéto-tellurique.

Block diagram of M.T. sounding equipment.

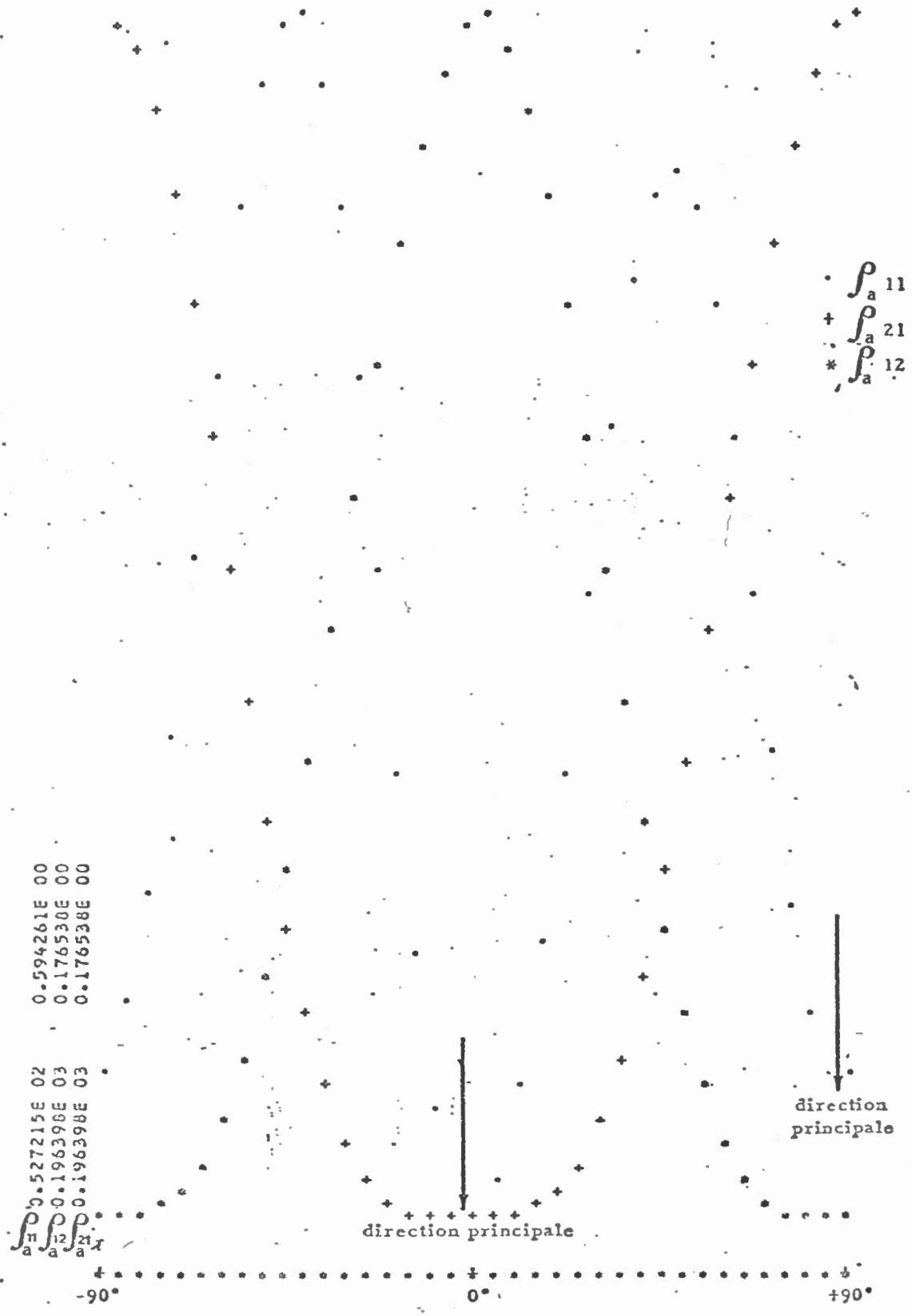

Figure 10: Exemple de rotation des axes de mesure pour la recherche des directions principales.

Example of measurement axes rotation for research of principal directions.

Figure 11: Organigramme du traitement tensoriel des données de S.M.T.

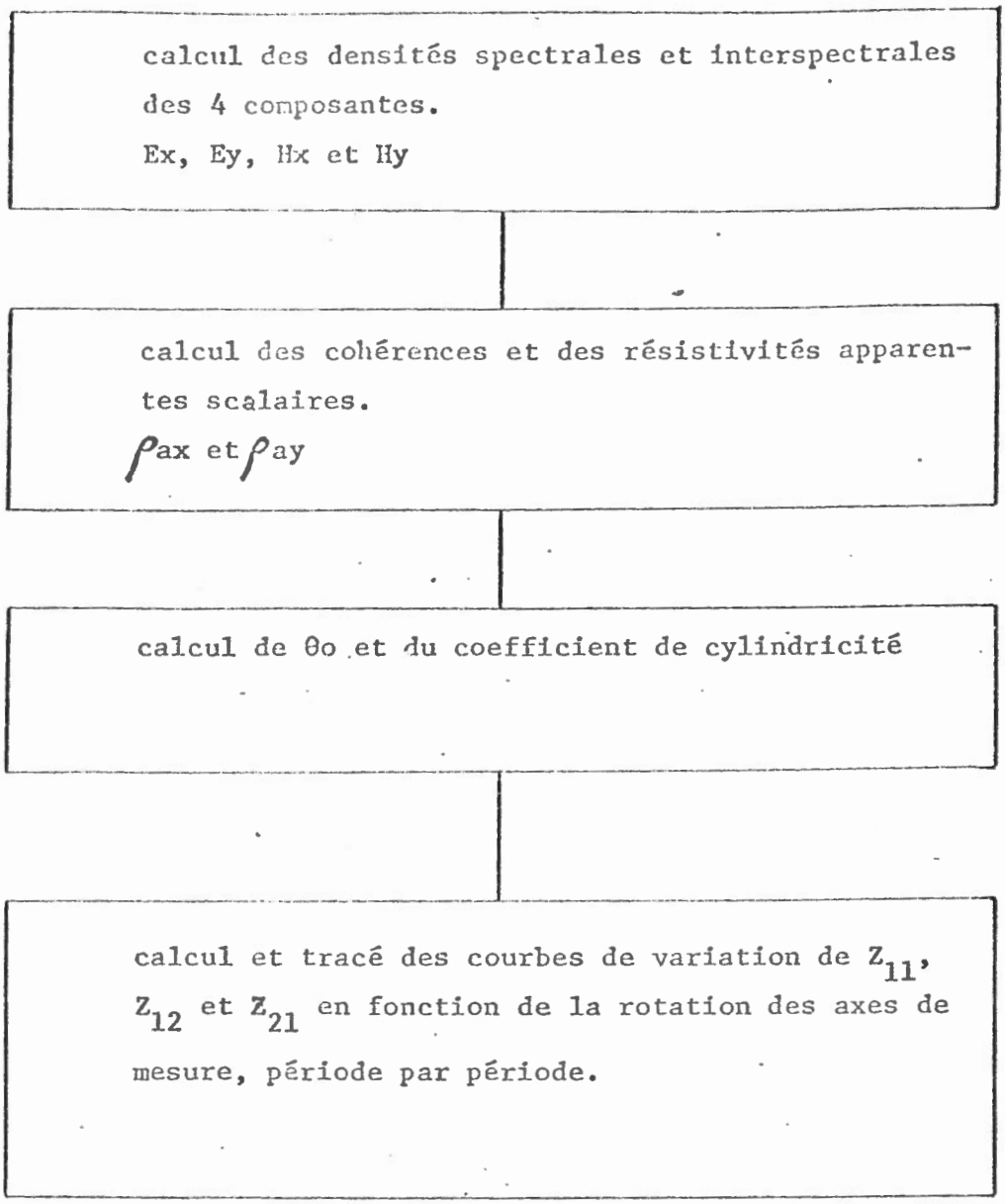

FIGURE 12 - RECONNAISSANCE M.T. LILLOOET

P. I - STATION I

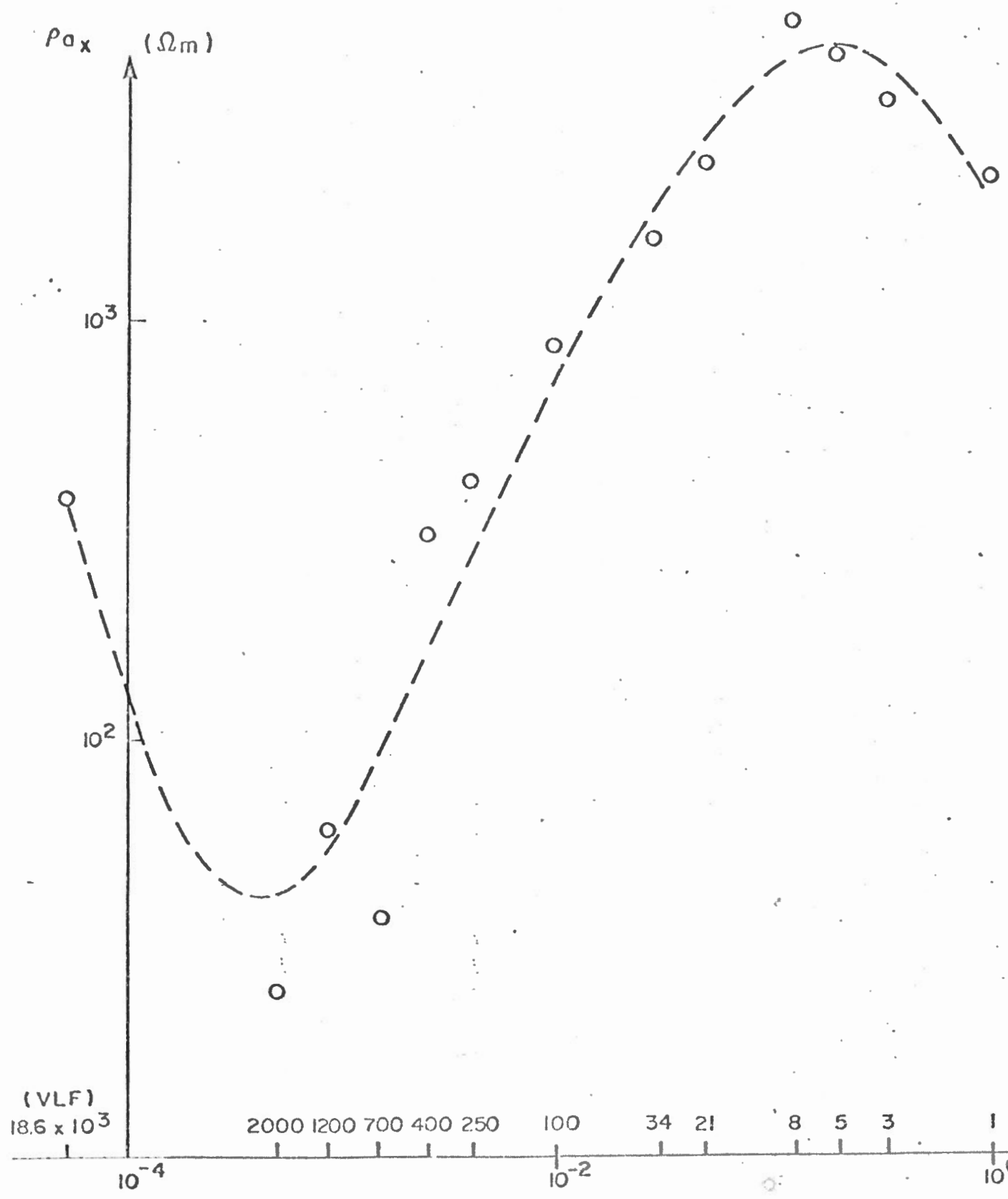

FIGURE 13 – RECONNAISSANCE M.T. LILLOOET

P. I – STATION 5

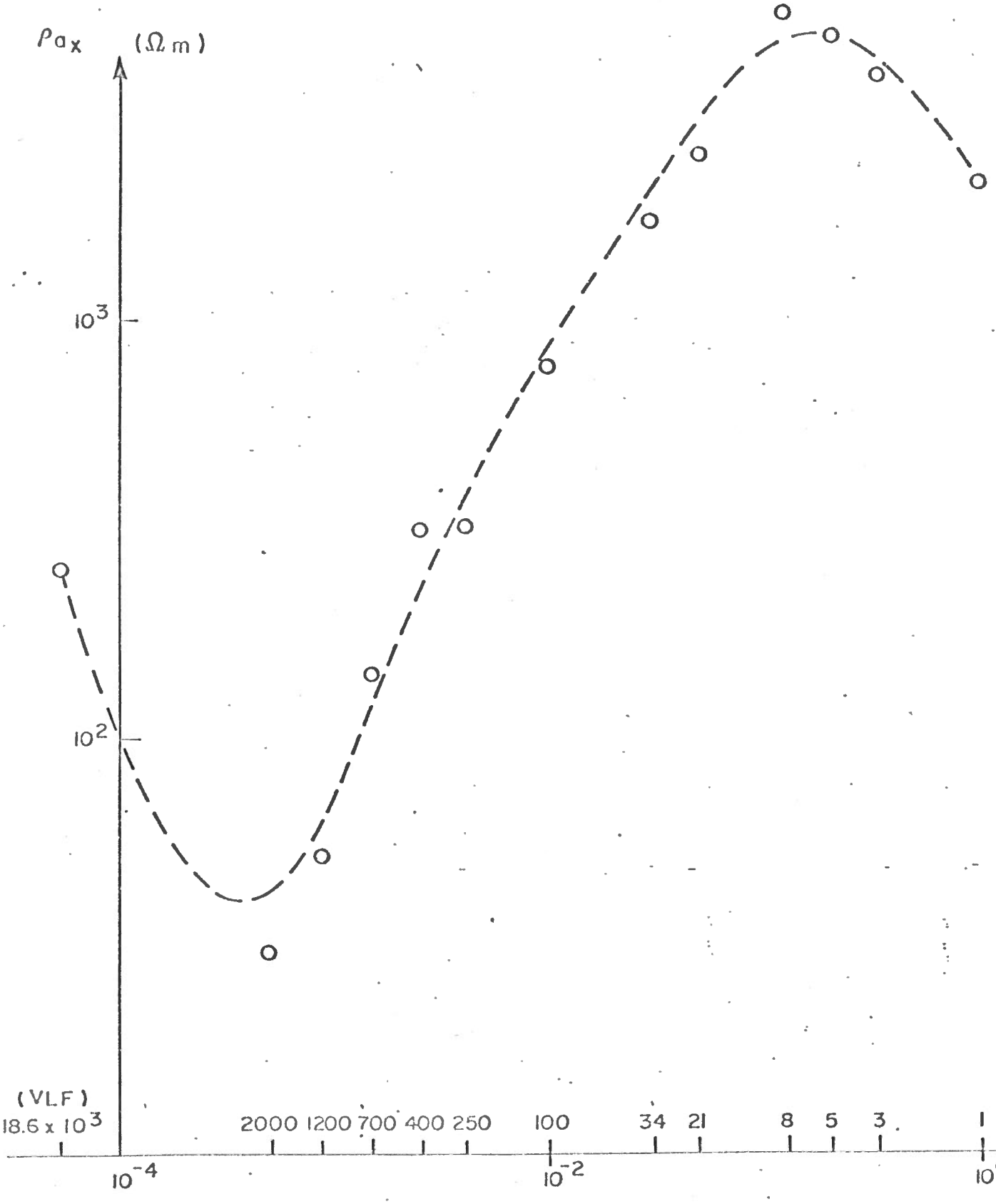

FIGURE 14 - RECONNAISSANCE M.T. LILLOOET

P. II - STATION I

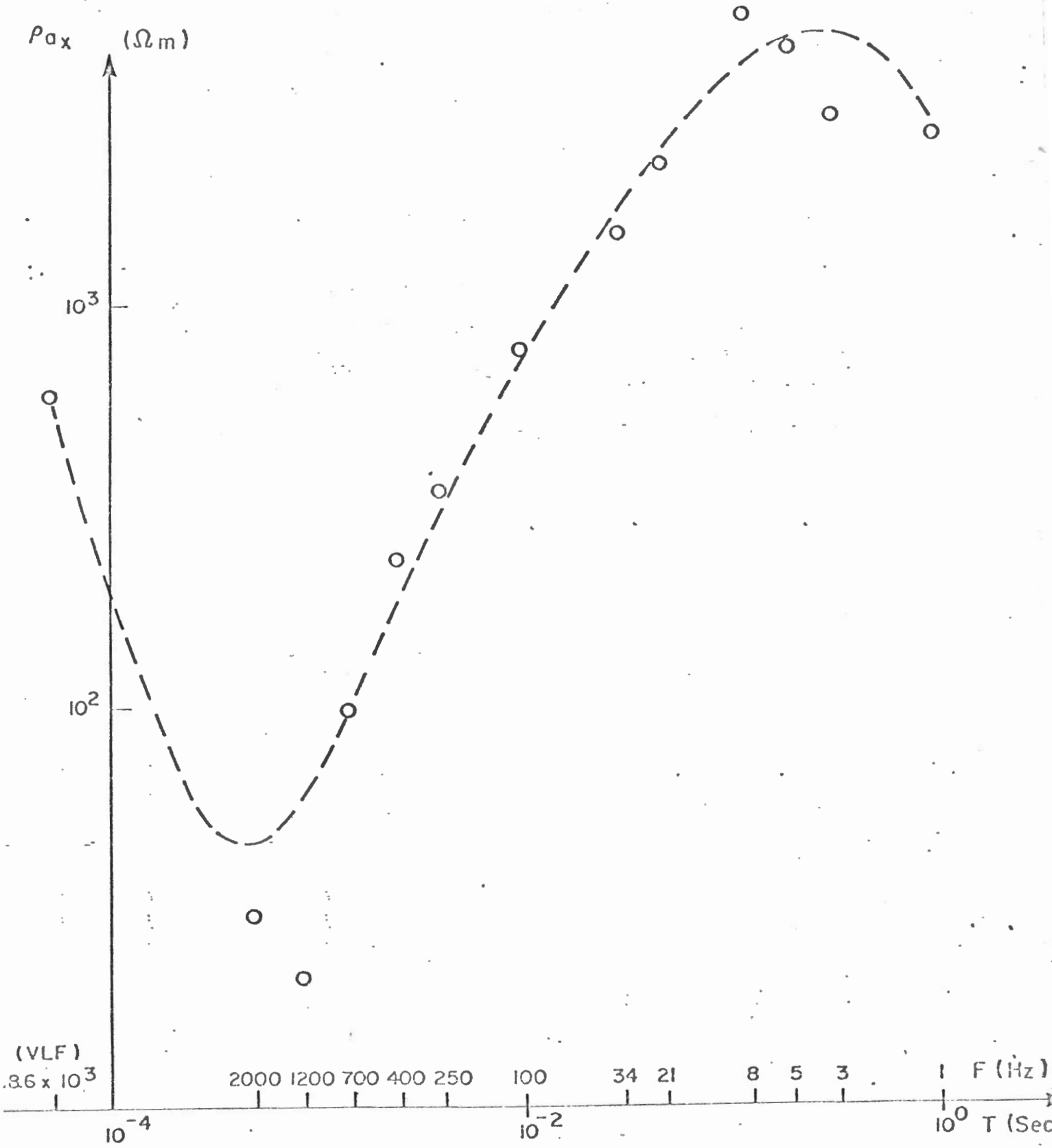

FIGURE 15 - RECONNAISSANCE M.T. LILLOOET

P. II - STATION 8

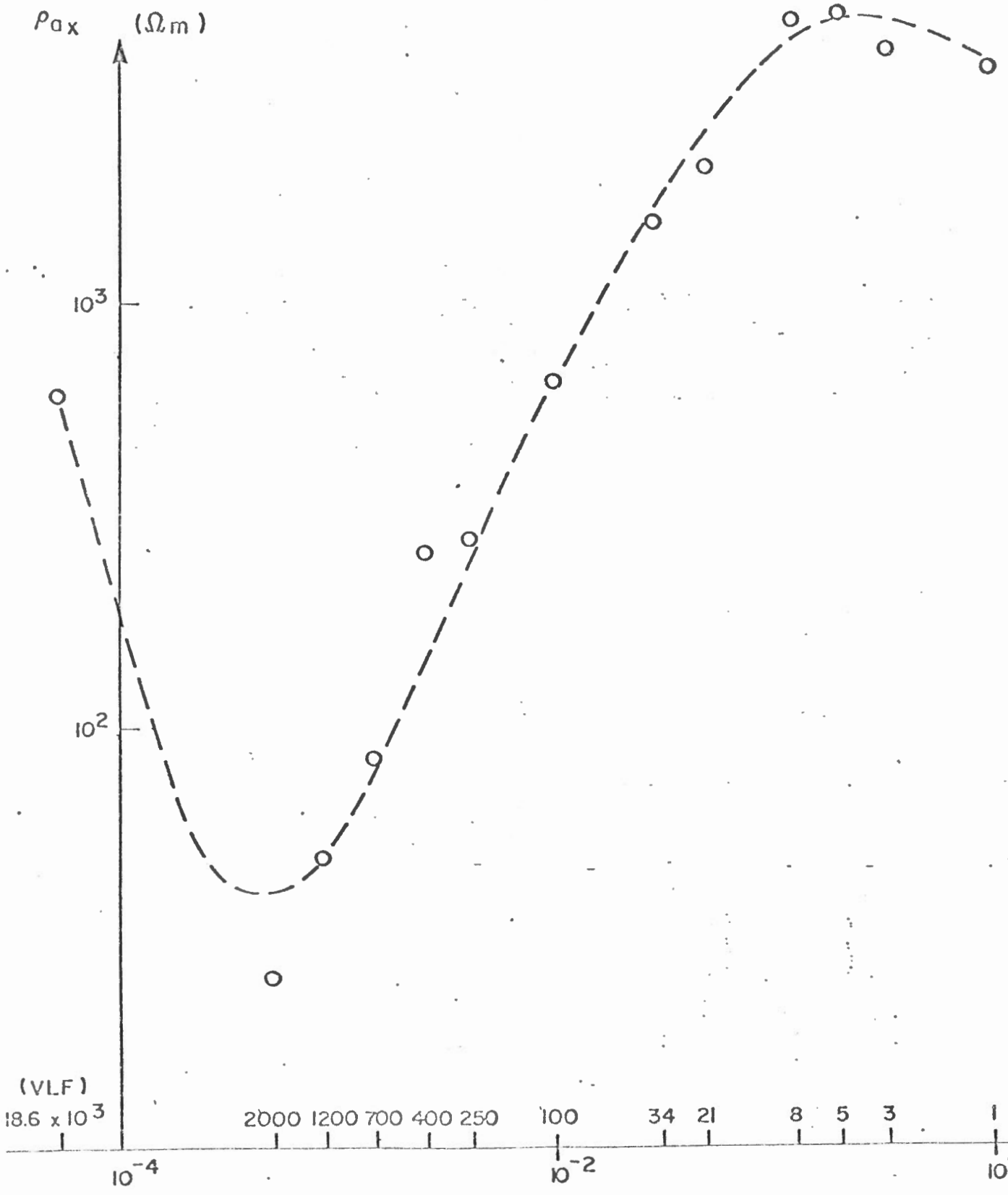

FIGURE 16 – RECONNAISSANCE M.T. LILLOOET

P. III – STATION I

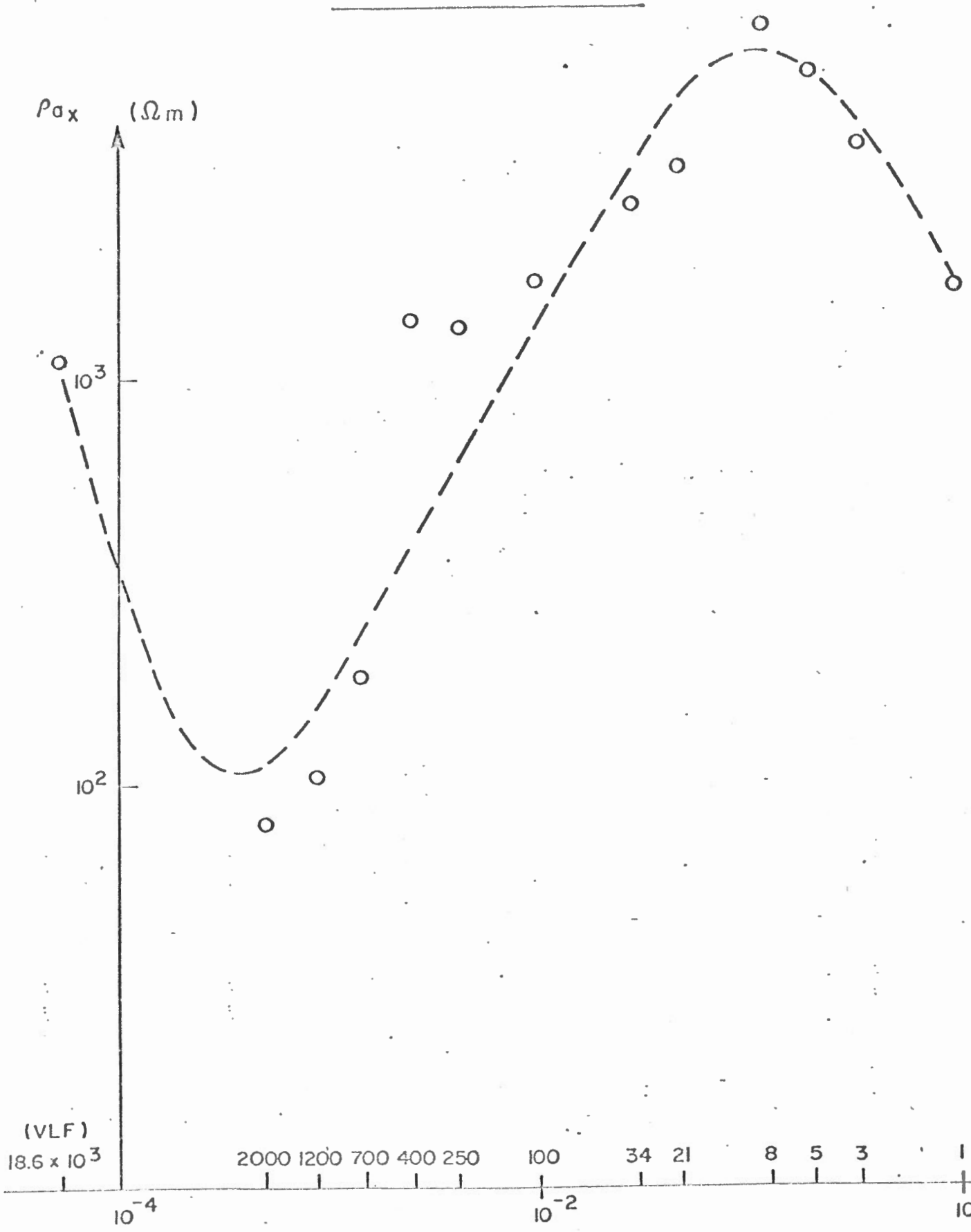

FIGURE 17 - RECONNAISSANCE M.T. LILLOOET

P. III - STATION 16

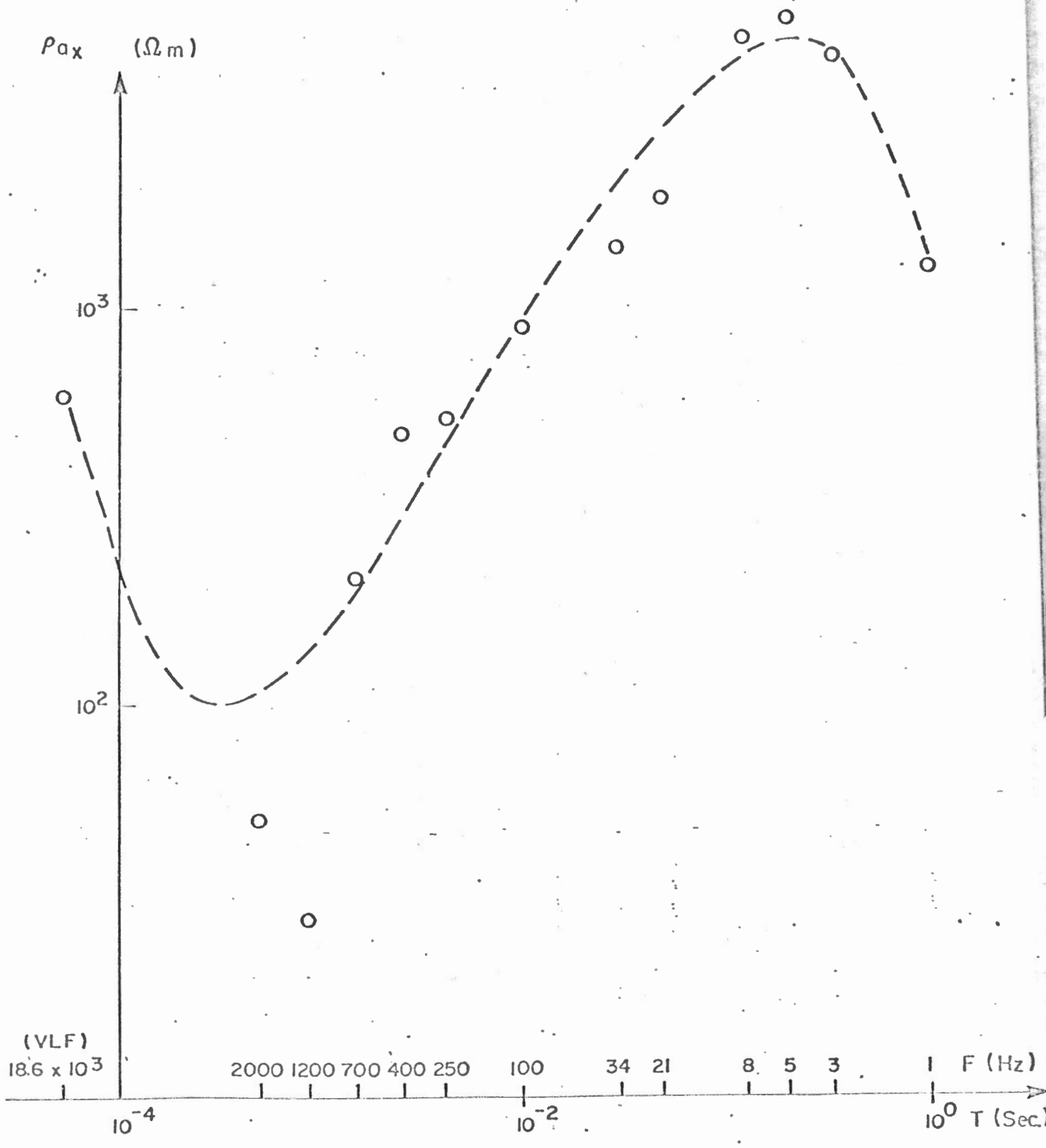

FIGURE 13 - RECONNAISSANCE M.T. LILLOOET

P. IV - STATION 1

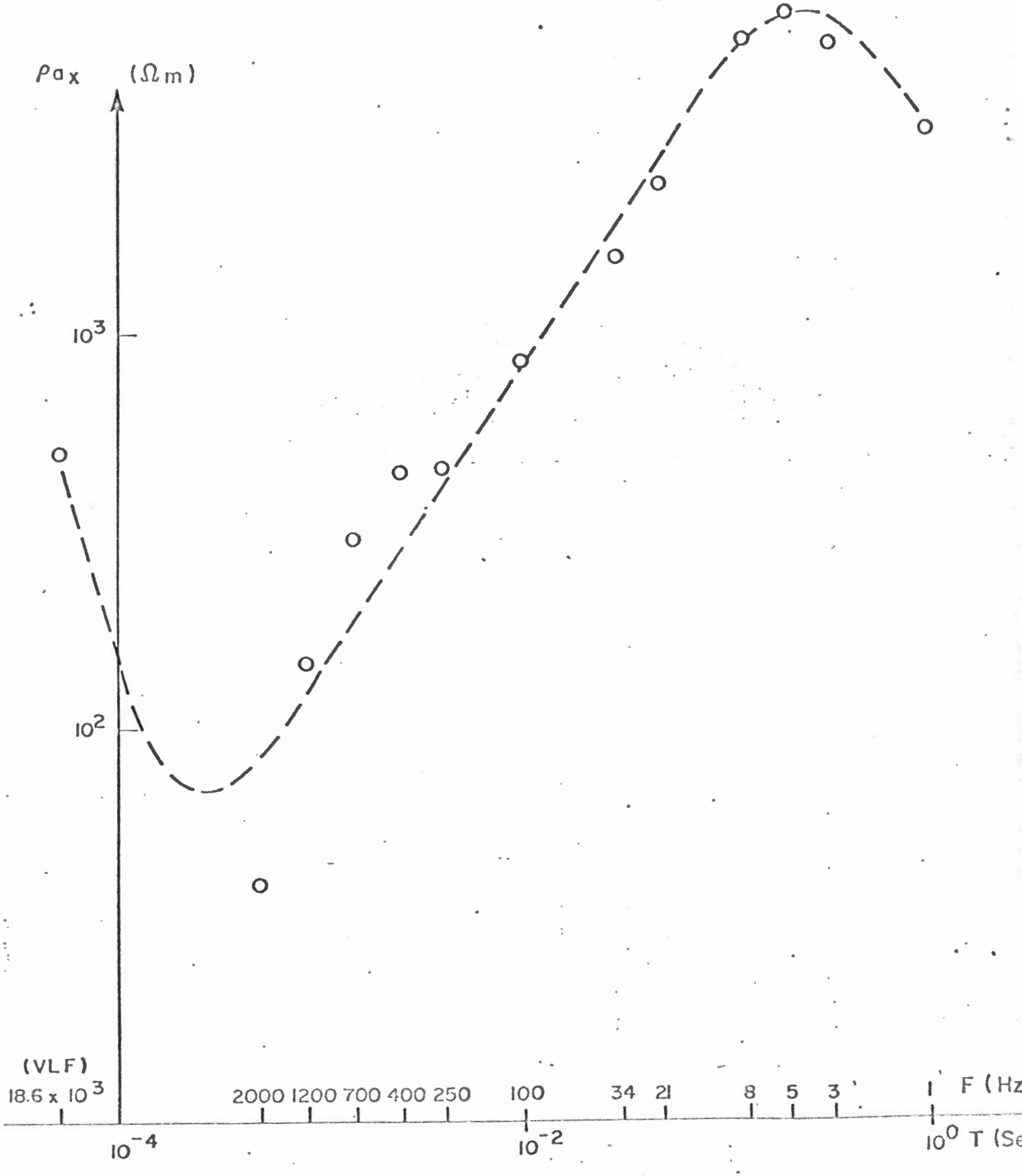

FIGURE 19 – RECONNAISSANCE M.T. LILLOOET

P. IV – STATION 6

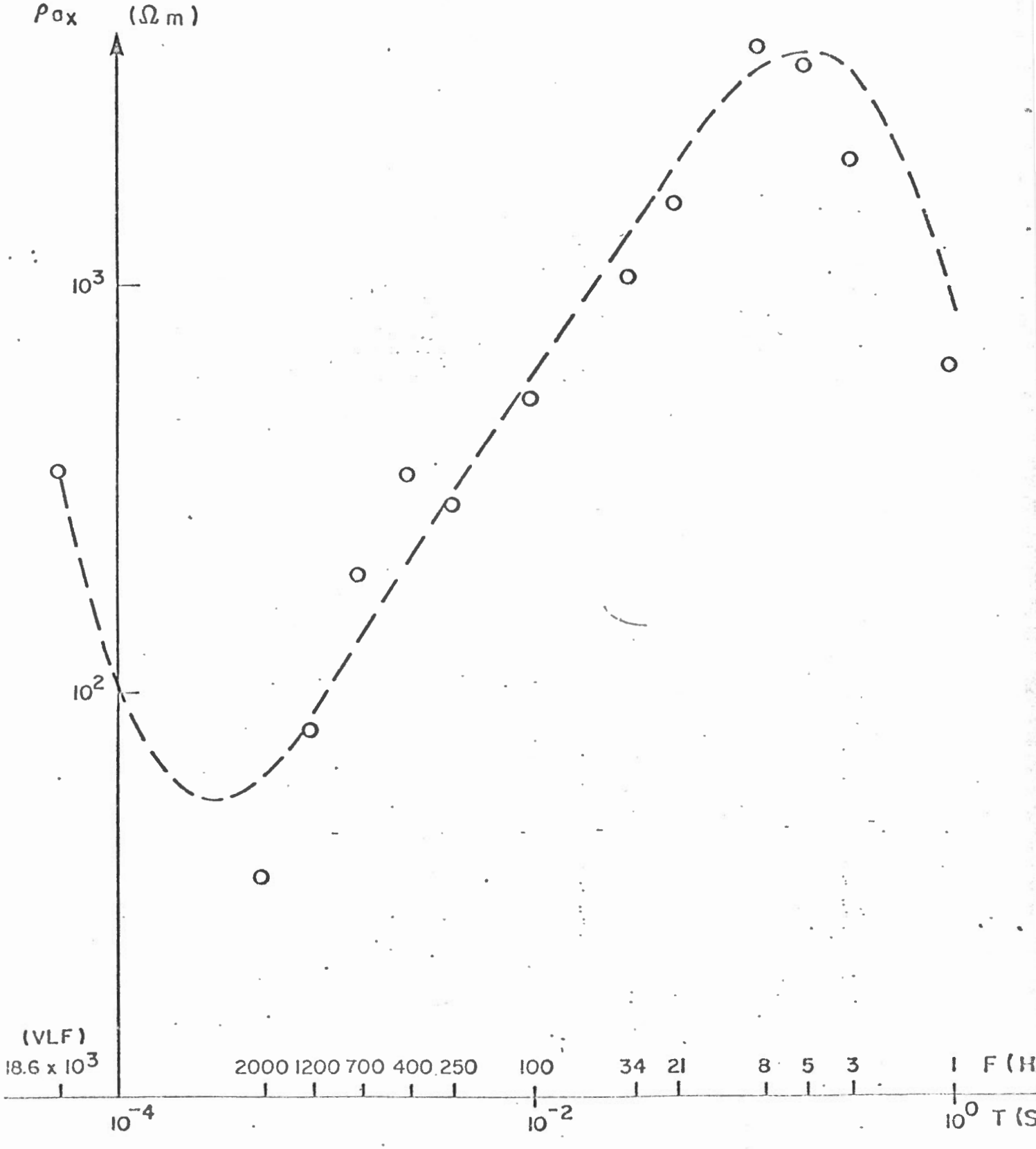

FIGURE 20 – RECONNAISSANCE M.T. LILLOOET

P.M.T. PROFIL / M.T.P. PROFILE P.I

PSEUDO-SECTION · ρ_{ax} (60° N.E. Mag.)

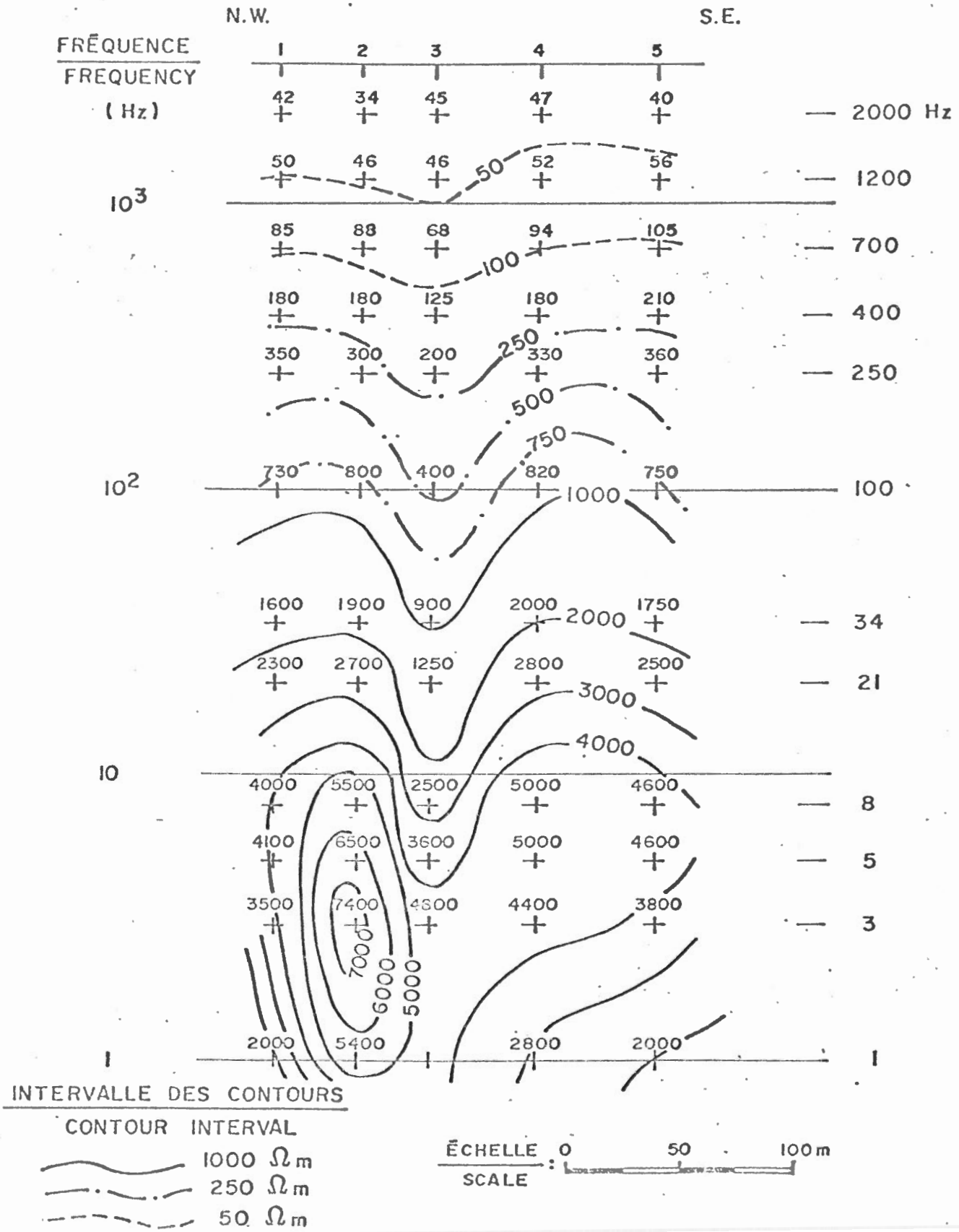

FIGURE II — RECONNAISSANCE M.T. SURVEY

P.M.T. PROFIL / M.T.P. PROFILE — P. II

PSEUDO-SECTION ρ_{ax} (60° N.E. Mag.)

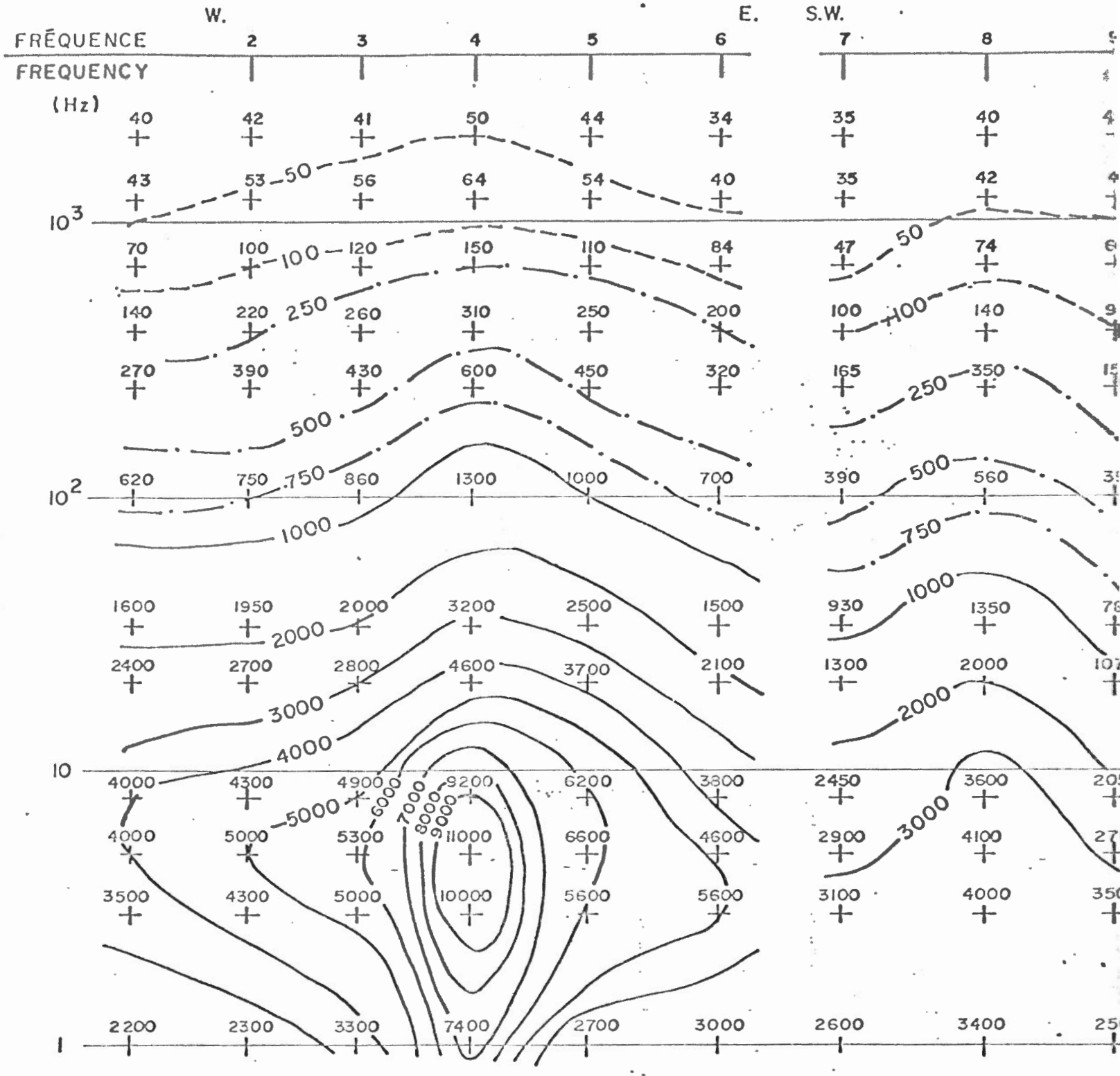

INTERVALLE DES CONTOURS
CONTOUR INTERVAL

1000 Ω m
250 Ω m
50 Ω m

ÉCHELLE 0 50 100
SCALE

FIGURE 22 - RECONNAISSANCE M.T. LILLOOET

P.M.T. PROFIL / M.T.P. PROFILE P. III

PSEUDO-SECTION ρ_{ax} (E.W. MAG.)

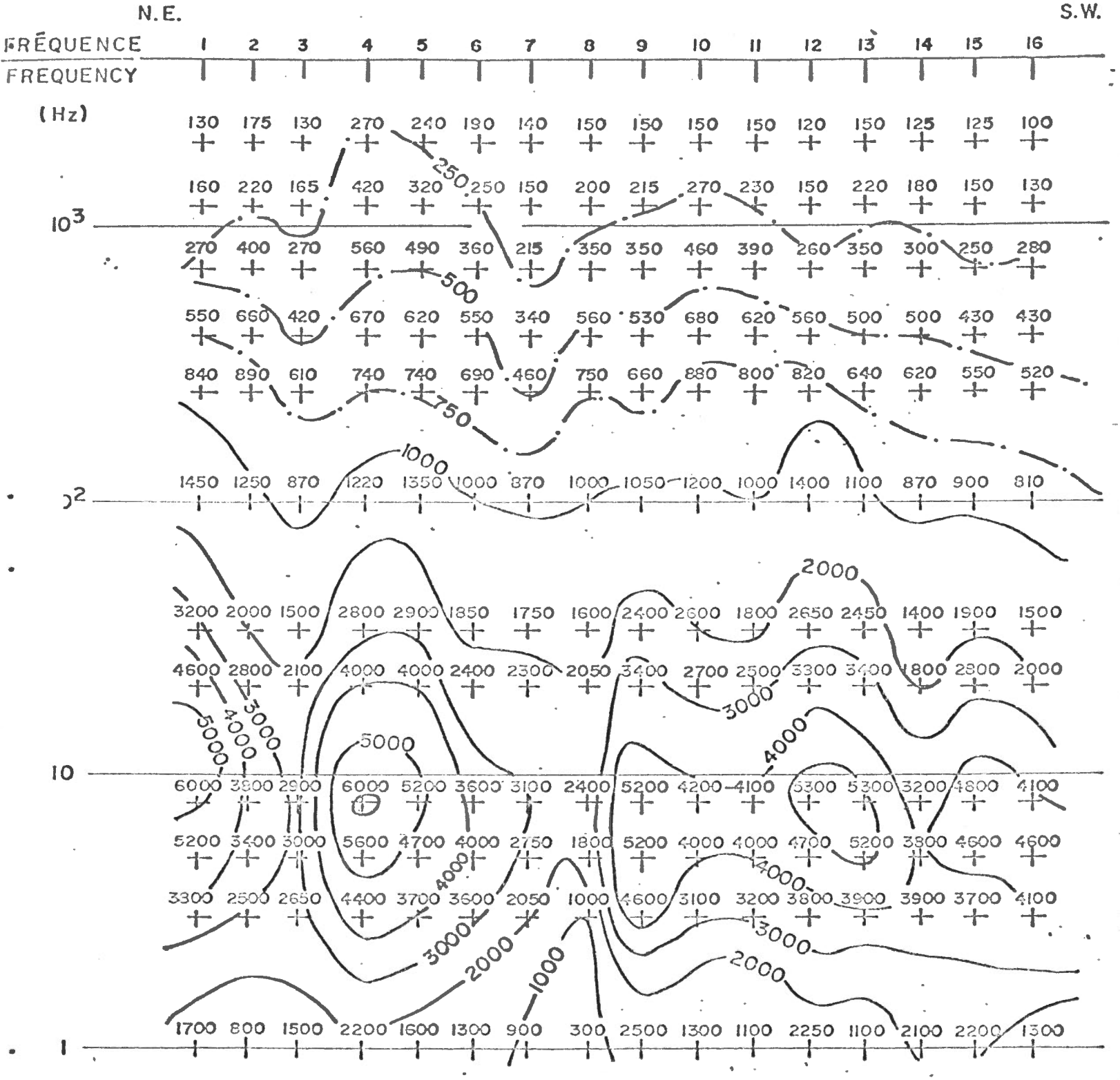

INTERVALLE DES CONTOURS / CONTOUR INTERVAL

1000 Ωm

250 Ωm

ÉCHELLE / SCALE : 0 100 200 m

FIGURE 23 — RECONNAISSANCE M.T. LILLOOET

P.M.T. PROFIL / M.T.P. PROFILE P. IV

PSEUDO-SECTION P_{ax} (E.W. MAG.)

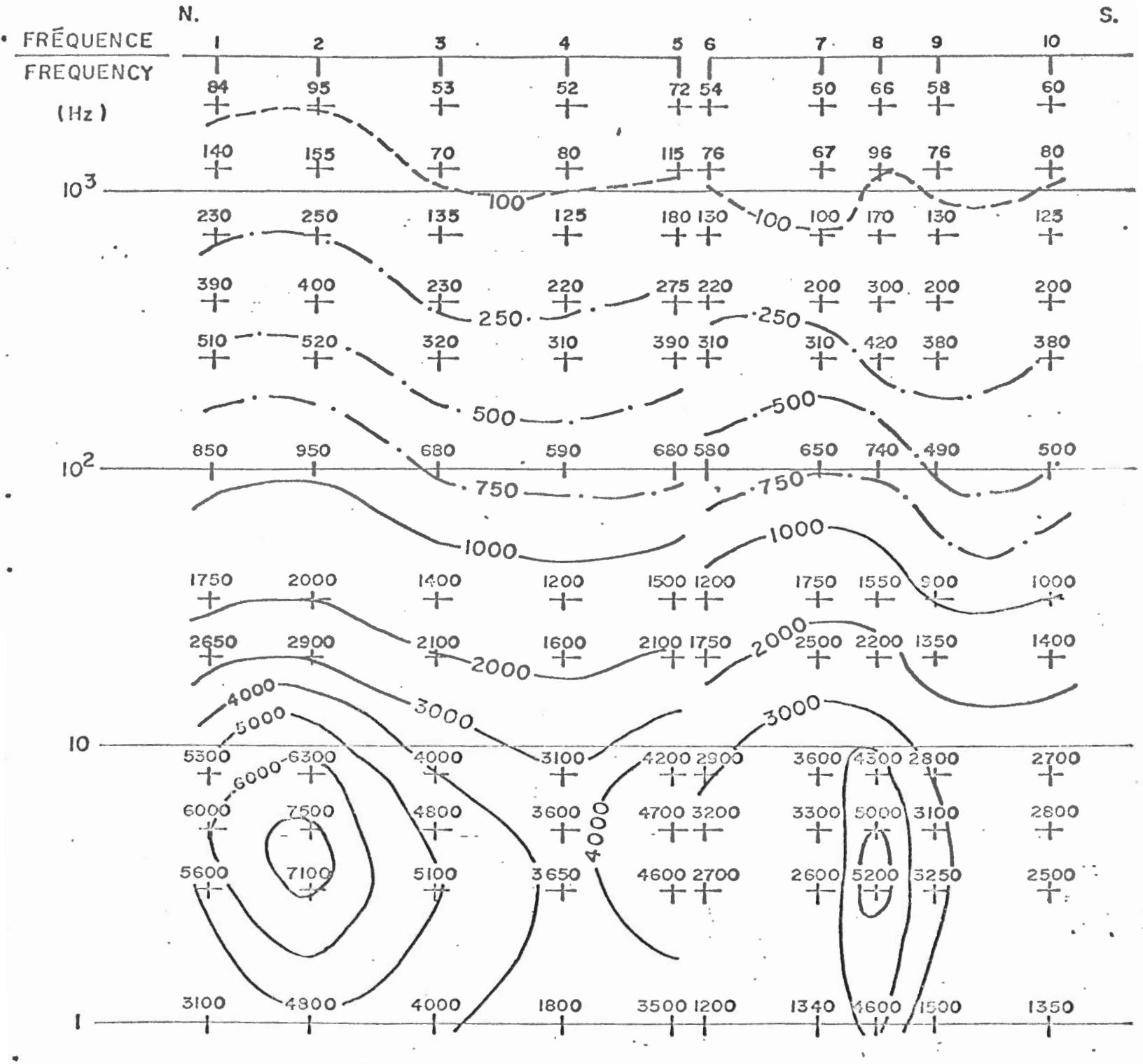

INTERVALLE DES CONTOURS
CONTOUR INTERVAL

1000 Ω m
250 Ω m
100 Ω m

ÉCHELLE / SCALE : 0 100 200 m

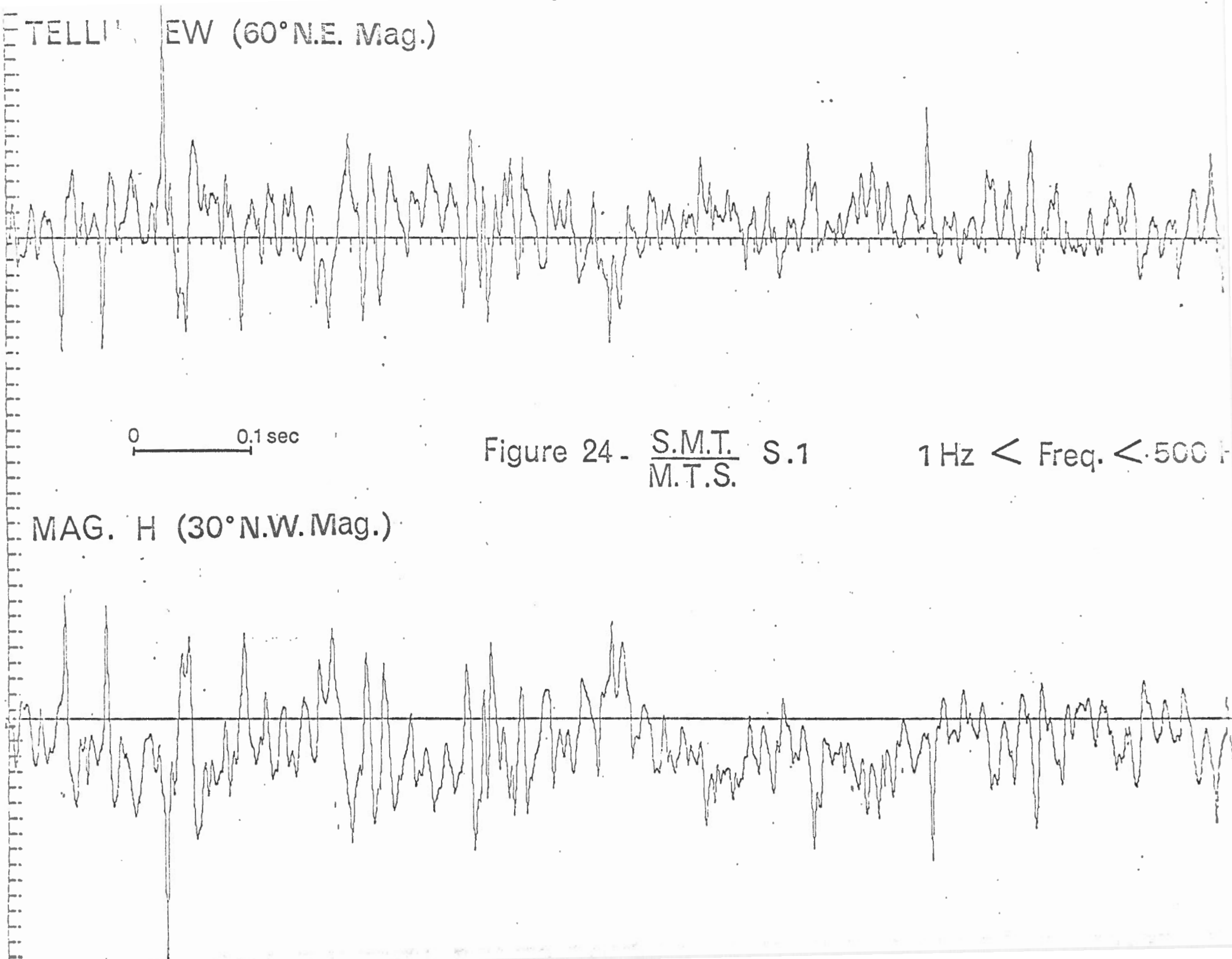

Figure 24 - $\frac{\text{S.M.T.}}{\text{M.T.S.}}$ S.1 1 Hz < Freq. < 500 H

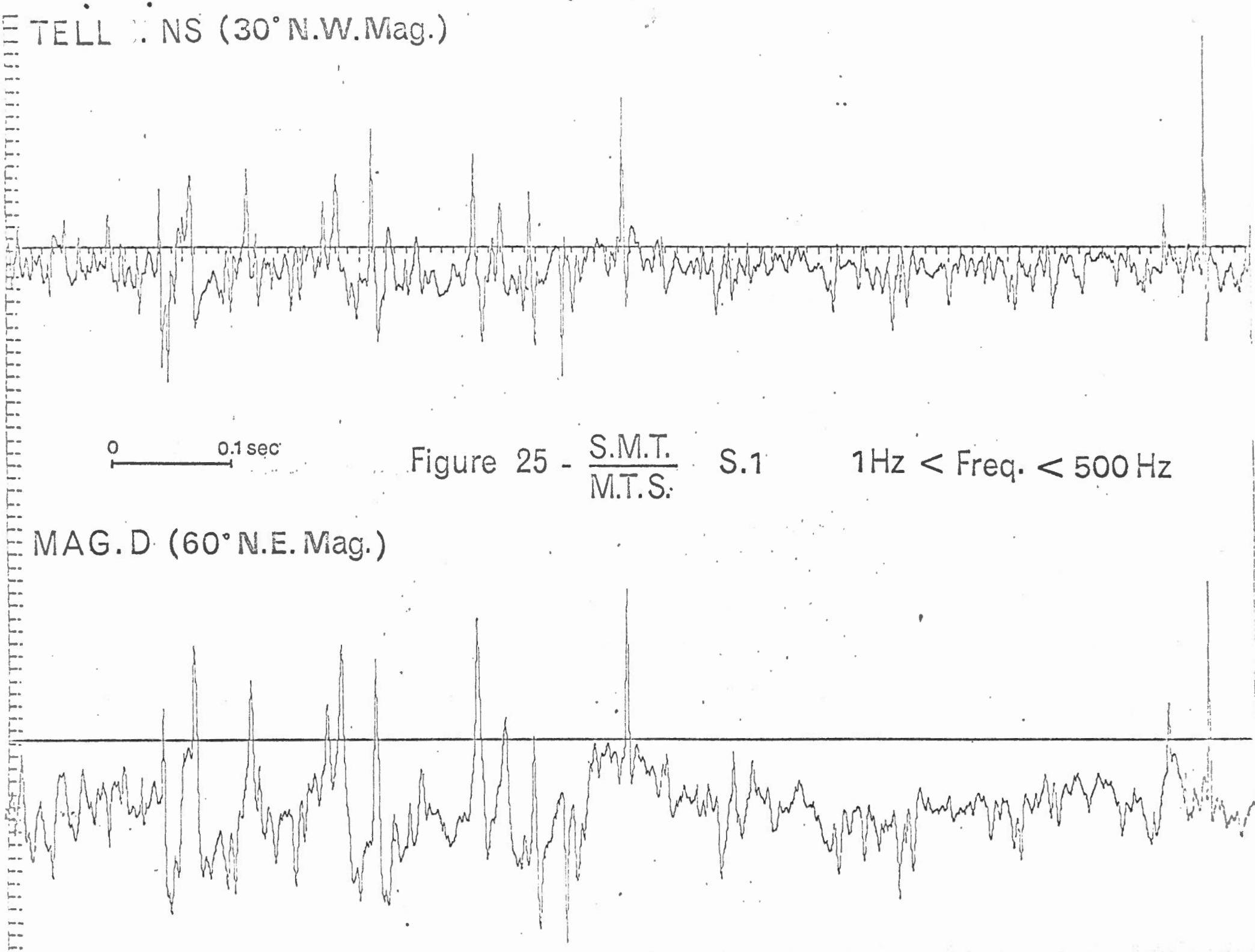

Figure 25 - $\frac{\text{S.M.T.}}{\text{M.T.S.}}$ S.1 1Hz < Freq. < 500 Hz

COHERENCE NS D

T	COH	T	COH	T	COH
0.0	G(1)= 0.100E 01	0.199E 01	G(2)= 0.100E 01	0.997E 00	G(3)= 0.591E 00
0.665E CC	G(4)= 0.920E 00	0.499E 00	G(5)= 0.984E 00	0.399E 00	G(6)= 0.989E 00
0.332E CC	G(7)= 0.965E 00	0.285E 00	G(8)= 0.952E 00	0.249E 00	G(9)= 0.939E 00
0.222E CC	G(10)= 0.931E 00	0.199E 00	G(11)= 0.925E 00	0.181E 00	G(12)= 0.920E 00
0.153E CC	G(13)= 0.887E 00	0.133E 00	G(14)= 0.842E 00	0.117E 00	G(15)= 0.816E 00
0.997E-01	G(16)= 0.772E 00	0.867E-01	G(17)= 0.786E 00	0.739E-01	G(18)= 0.816E 00
0.623E-01	G(19)= 0.795E 00	0.525E-01	G(20)= 0.757E 00	0.443E-01	G(21)= 0.783E 00
0.376E-01	G(22)= 0.816E 00	0.317E-01	G(23)= 0.800E 00	0.266E-01	G(24)= 0.801E 00
0.224E-01	G(25)= 0.735E 00	0.188E-01	G(26)= 0.739E 00	0.157E-01	G(27)= 0.781E 00
0.131E-01	G(28)= 0.801E 00	0.110E-01	G(29)= 0.829E 00	0.915E-02	G(30)= 0.844E 00
0.764E-02	G(31)= 0.887E 00	0.637E-02	G(32)= 0.893E 00	0.532E-02	G(33)= 0.878E 00
0.444E-02	G(34)= 0.835E 00	0.371E-02	G(35)= 0.258E-01	0.309E-02	G(36)= 0.256E-01

C.1C0000E C1 0.256337E-01

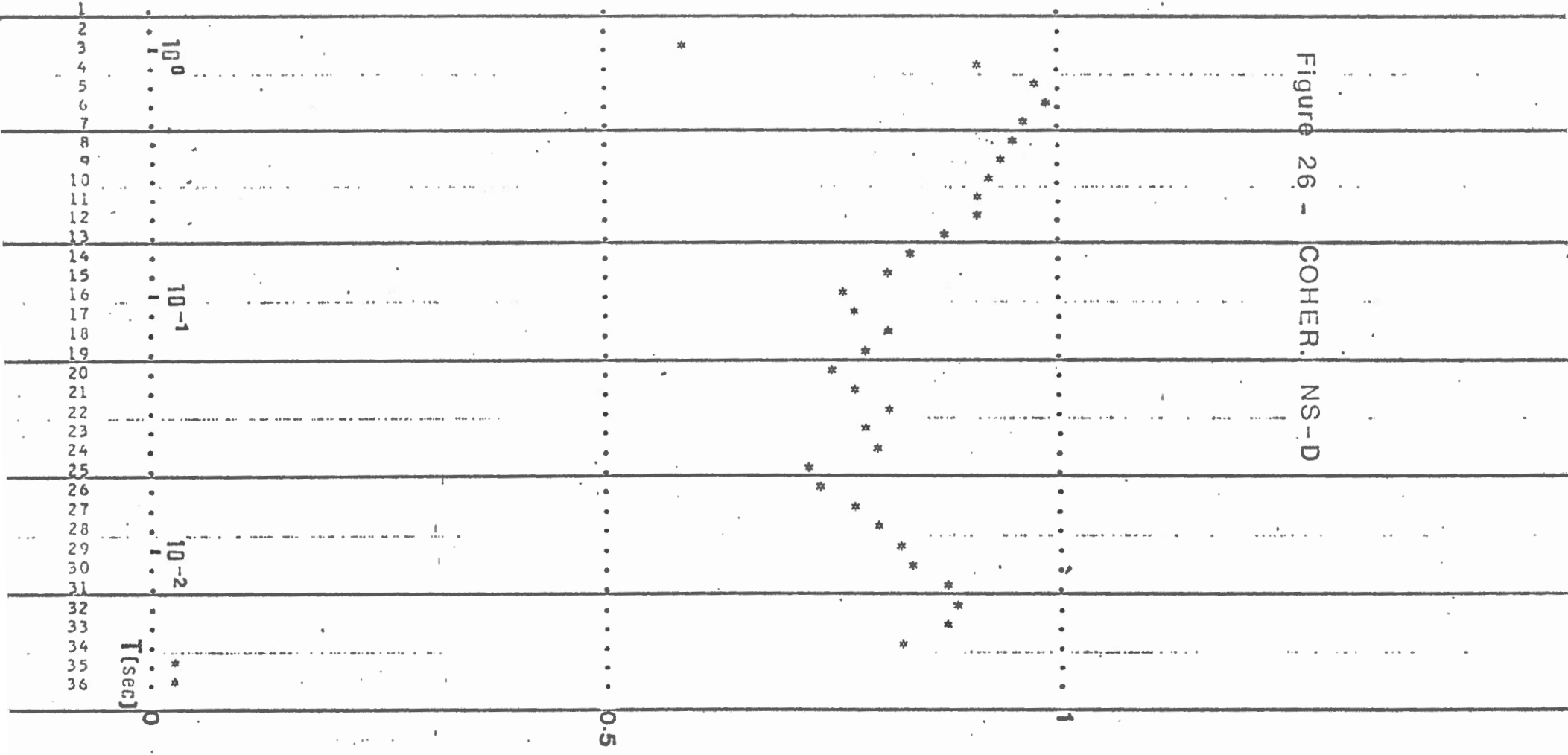

Figure 26 - COHER. NS-D

COHERENCE EW H

T	COH	T	COH	T	COH
0.0	G(1)= 0.100E 01	0.199E 01	G(2)= 0.100E 01	0.997E 00	G(3)= 0.688E 00
0.665E CC	G(4)= 0.279E 00	0.499E 00	G(5)= 0.775E 00	0.399E 00	G(6)= 0.970E 00
0.332E CC	G(7)= 0.819E 00	0.285E 00	G(8)= 0.823E 00	0.249E 00	G(9)= 0.928E 00
0.222E 00	G(10)= 0.929E 00	0.199E 00	G(11)= 0.938E 00	0.181E 00	G(12)= 0.933E 00
0.153E C0	G(13)= 0.927E 00	0.133E 00	G(14)= 0.950E 00	0.117E 00	G(15)= 0.966E 00
0.997E-C1	G(16)= 0.968E 00	0.867E-01	G(17)= 0.980E 00	0.739E-01	G(18)= 0.983E 00
0.623E-C1	G(19)= 0.984E 00	0.525E-01	G(2C)= 0.986E 00	C.443E-01	G(21)= 0.989E 00
0.376E-01	G(22)= 0.988E 00	0.317E-01	G(23)= C.988E 00	0.266E-01	G(24)= 0.990E 00
0.224E-01	G(25)= 0.995E 00	0.188E-01	G(26)= 0.996E 00	0.157E-01	G(27)= 0.995E 00
0.131E-01	G(28)= 0.994E 00	0.110E-01	G(29)= 0.992E 00	0.915E-02	G(30)= 0.989E 00
0.764E-02	G(31)= 0.984E 00	0.637E-02	G(32)= 0.978E 00	0.532E-02	G(33)= 0.968E 00
0.444E-02	G(34)= 0.931E 00	0.371E-02	G(35)= 0.5C1E-01	0.309E-02	G(36)= 0.455E-01

C.1C0C00E C1 0.455369E-01

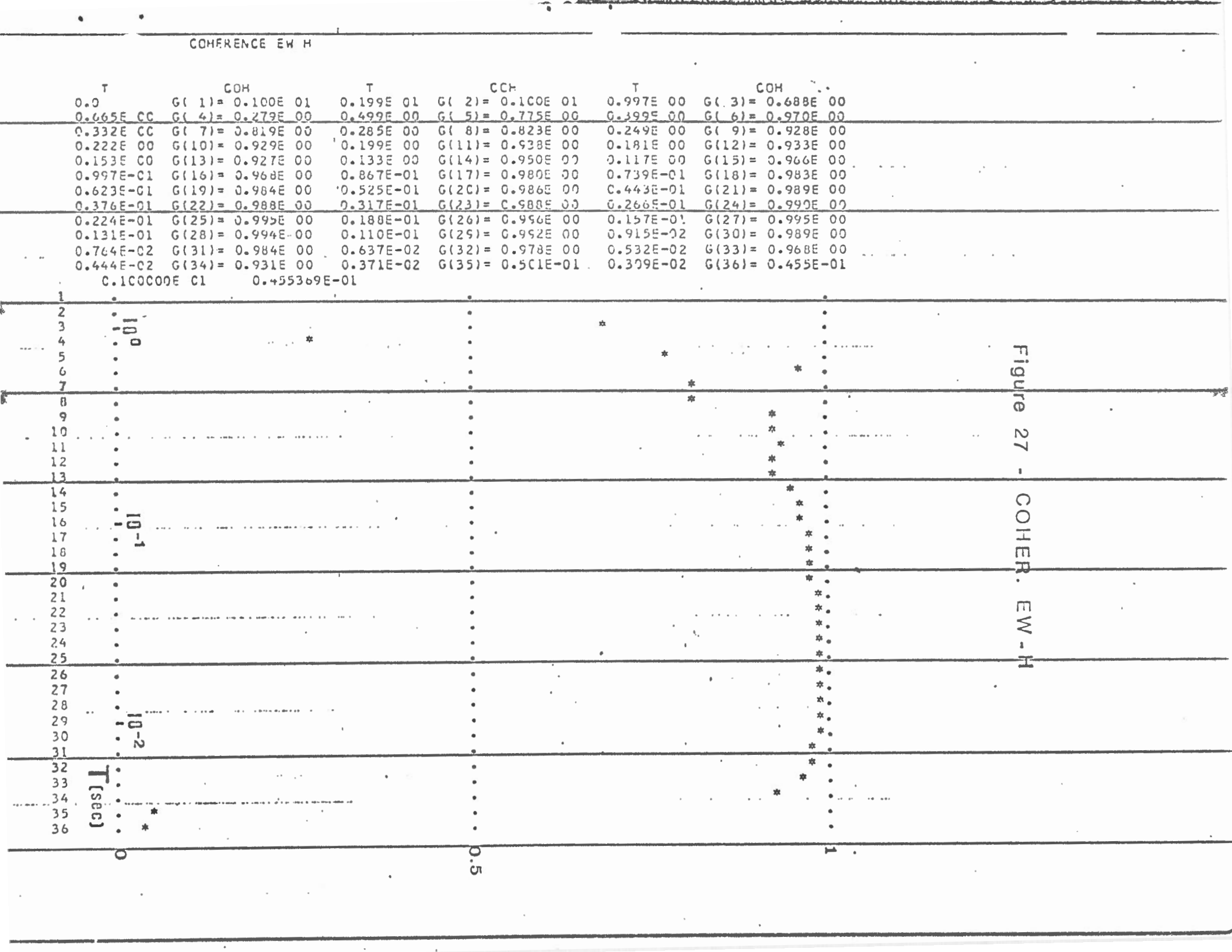

Figure 27 - COHER. EW - H

FIGURE 28 – RECONNAISSANCE M.T. LILLOOET

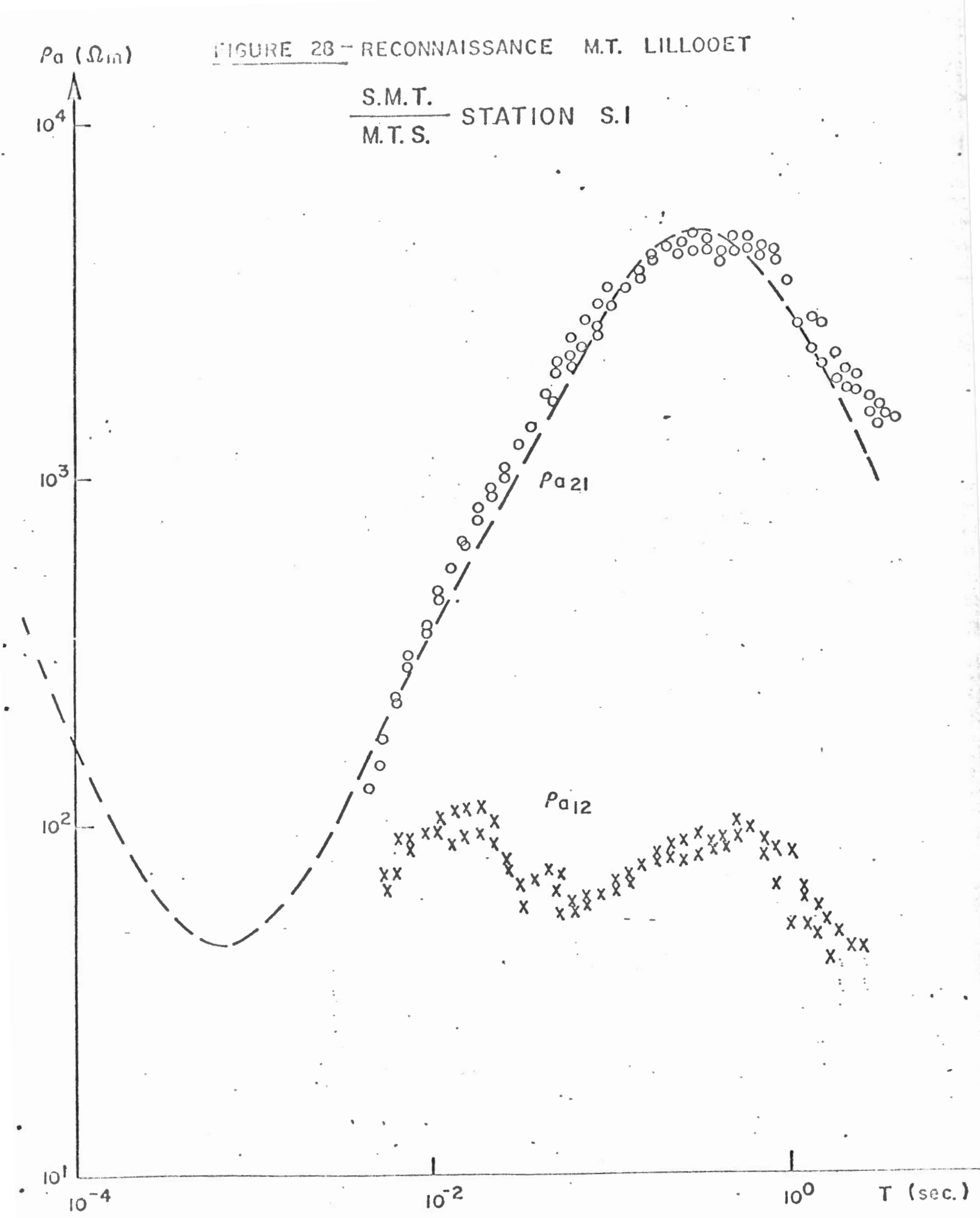

FIGURE 29 — RECONNAISSANCE M.T. LILLOOET

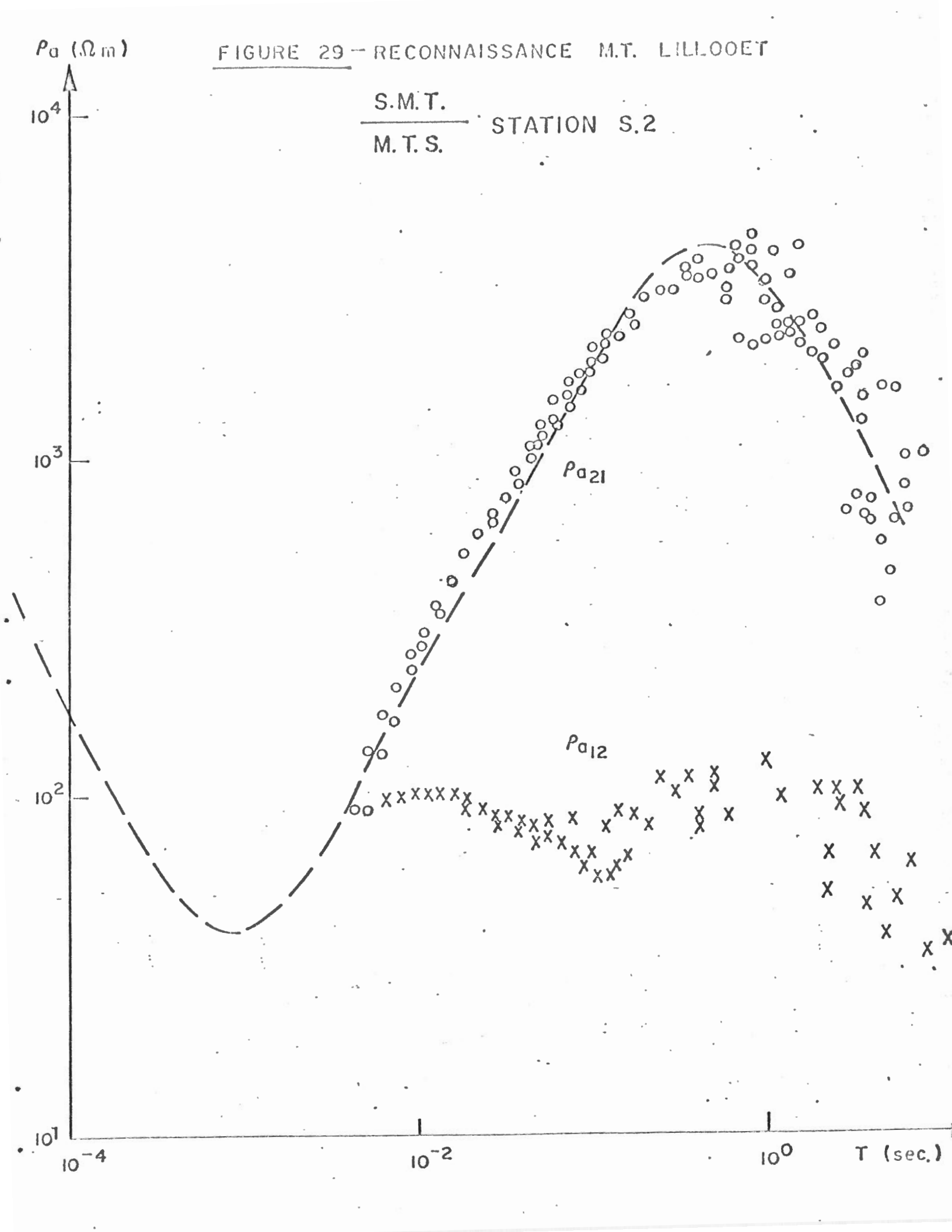

FIGURE 30 – RECONNAISSANCE M.T. LILLOOET

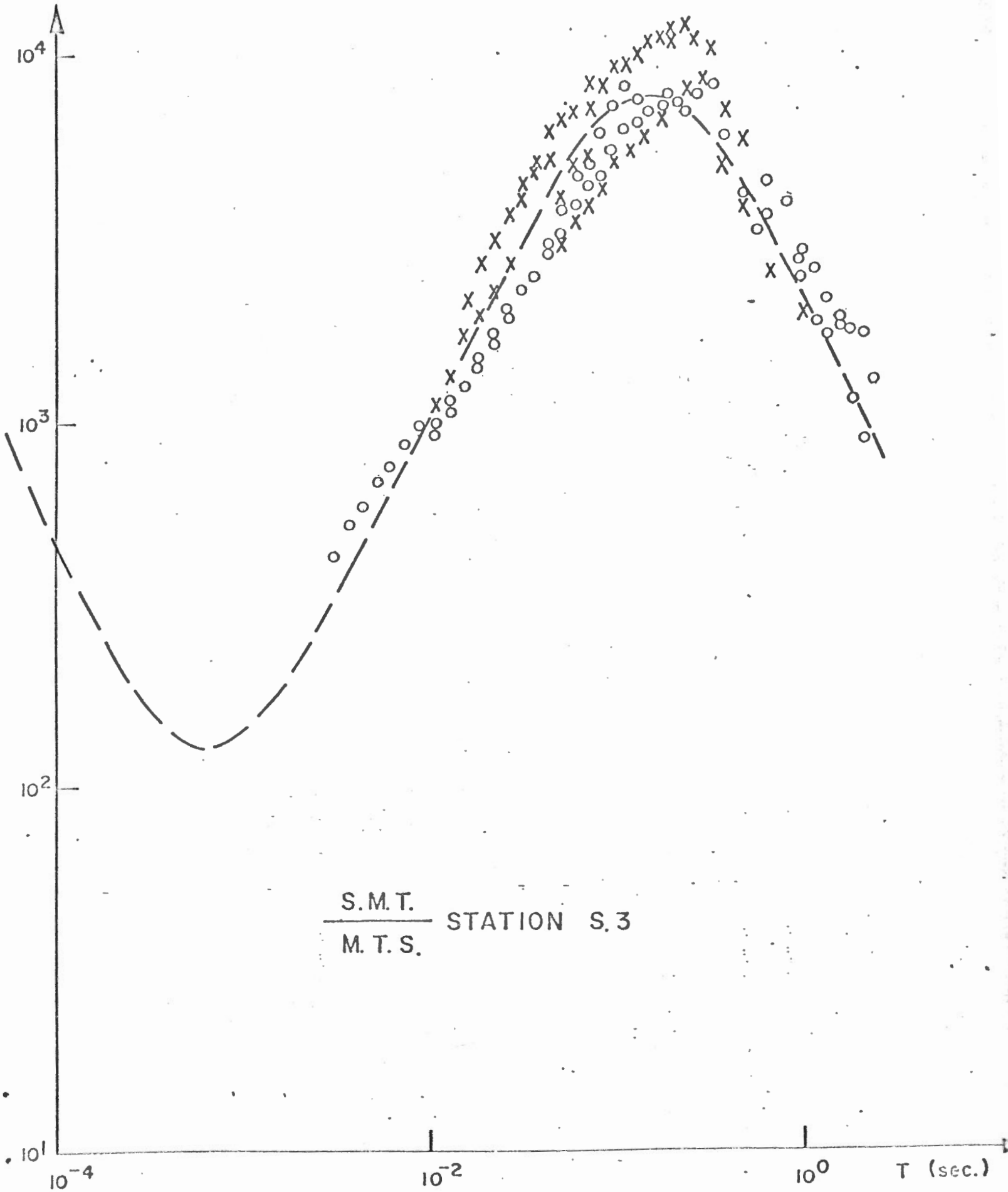

FIGURE 31 – RECONNAISSANCE M.T. LILLOOET

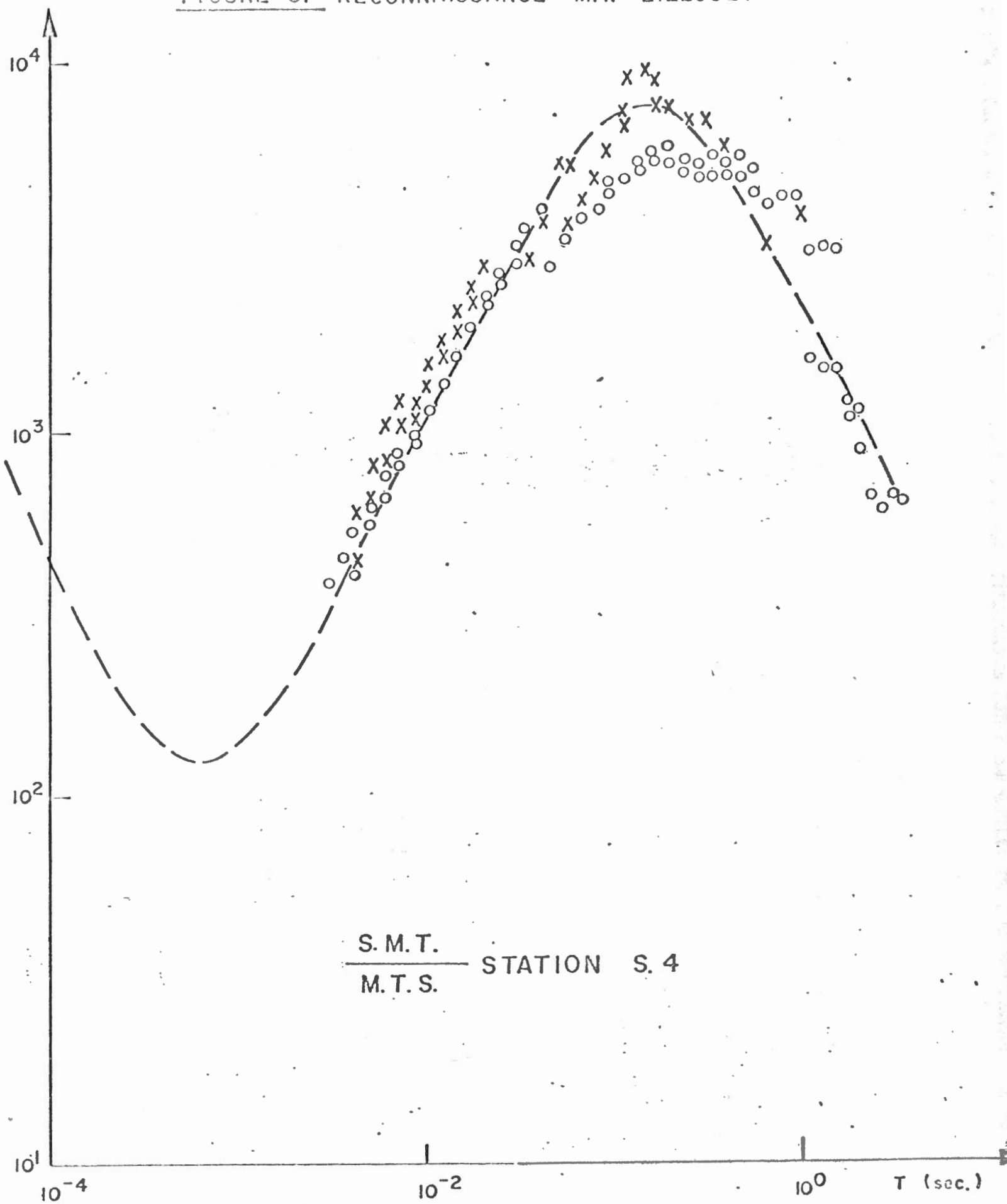

FIGURE 33 - DIRECTION PRINCIPALE / PRINCIPAL DIRECTION θ_{12}

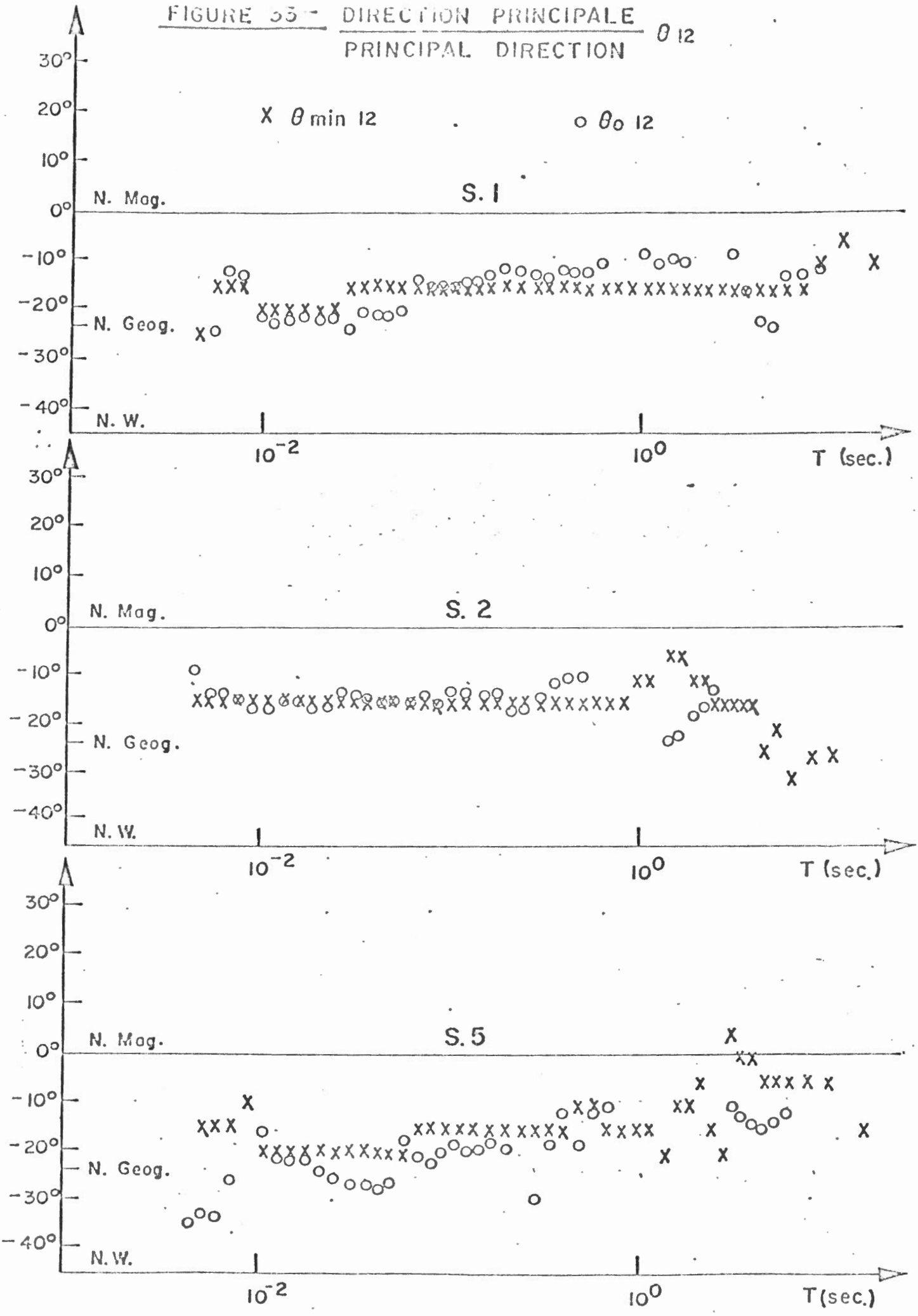

Figure 34: Courbes de sondage théorique au-dessus d'une structure à deux dimensions.

Theoretical M.T. sounding curves above a bidimensional structure.

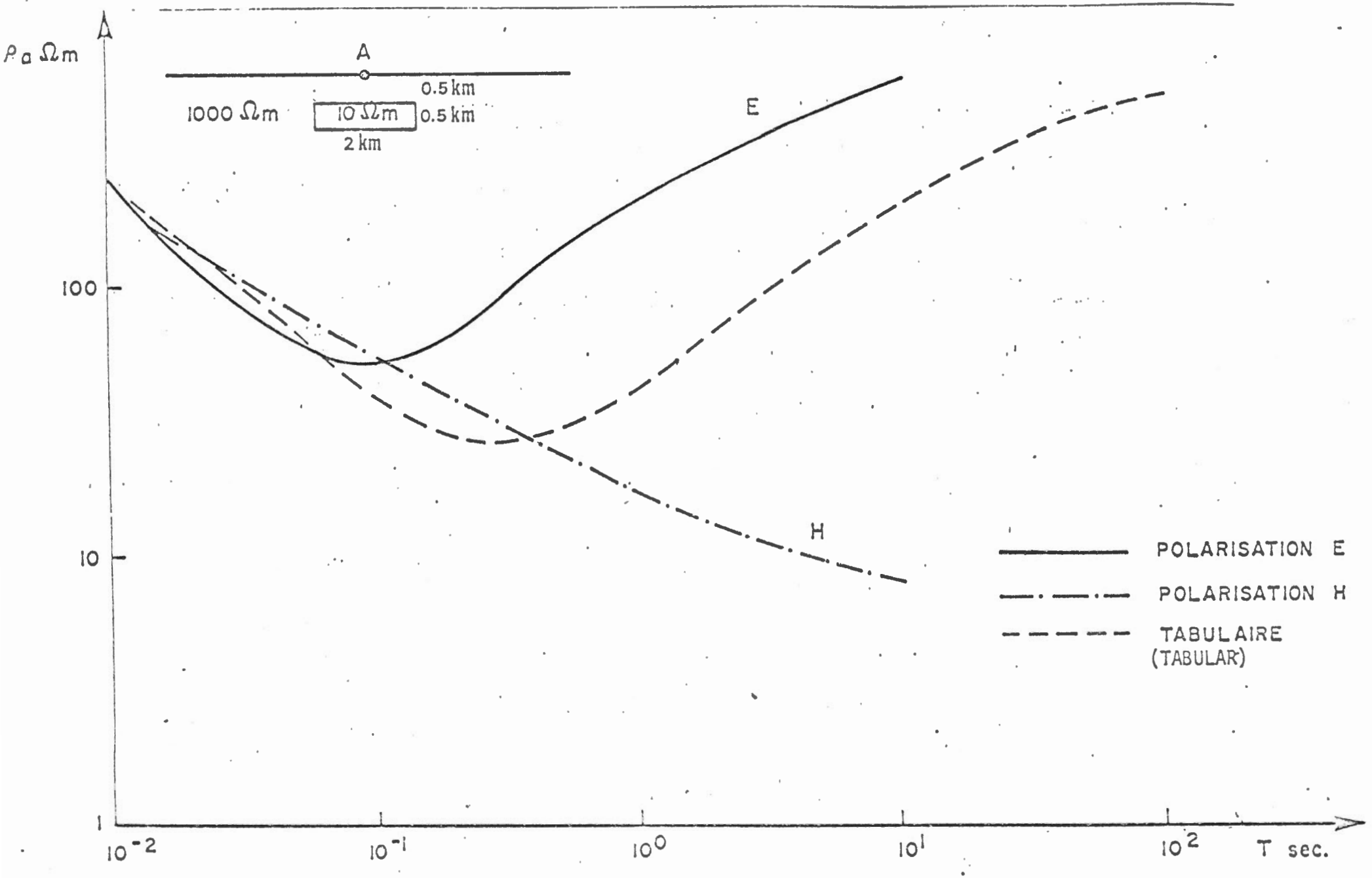

FIGURE 35 – DIRECTION LONGITUDINALE / LONGITUDINAL DIRECTION β_o

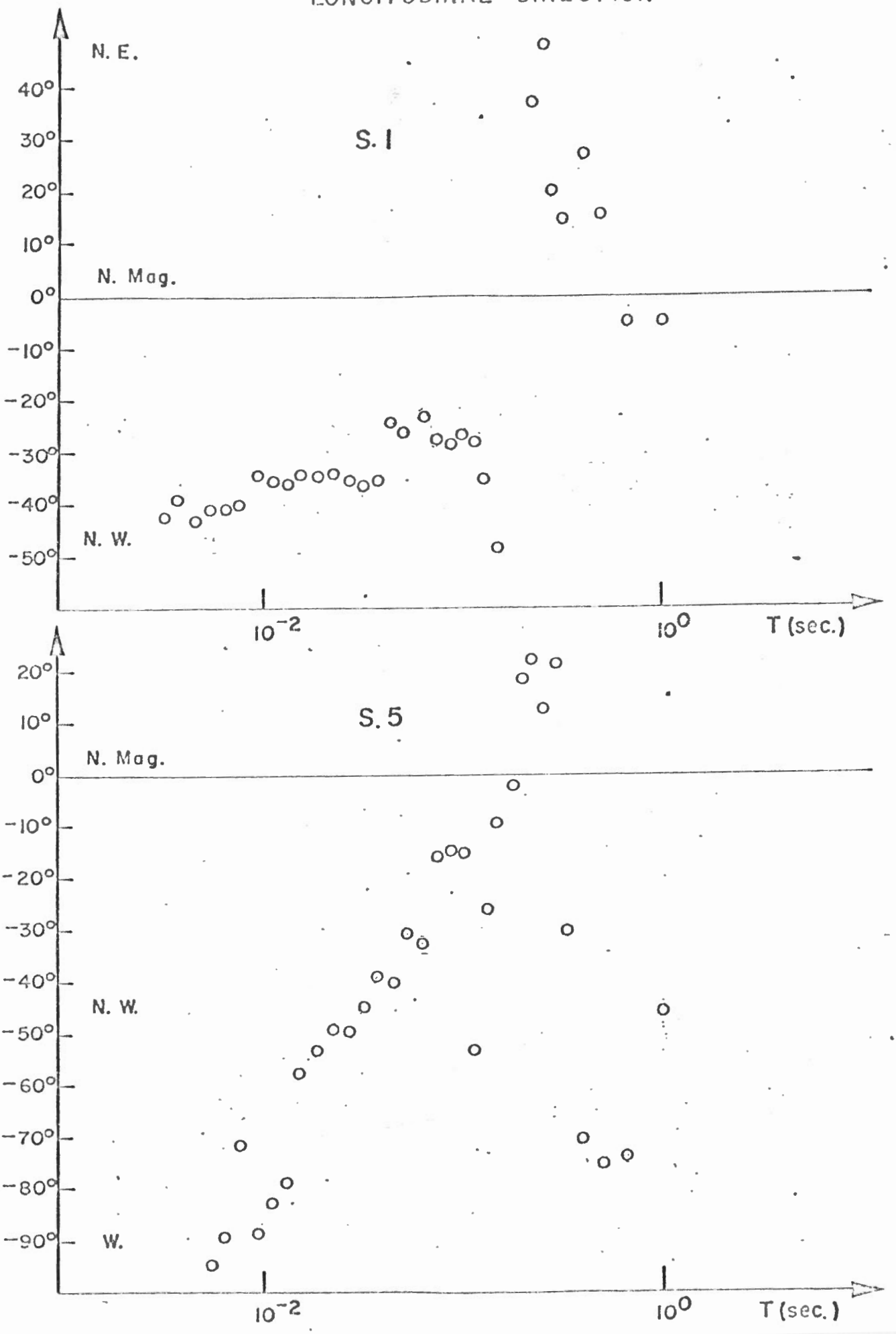

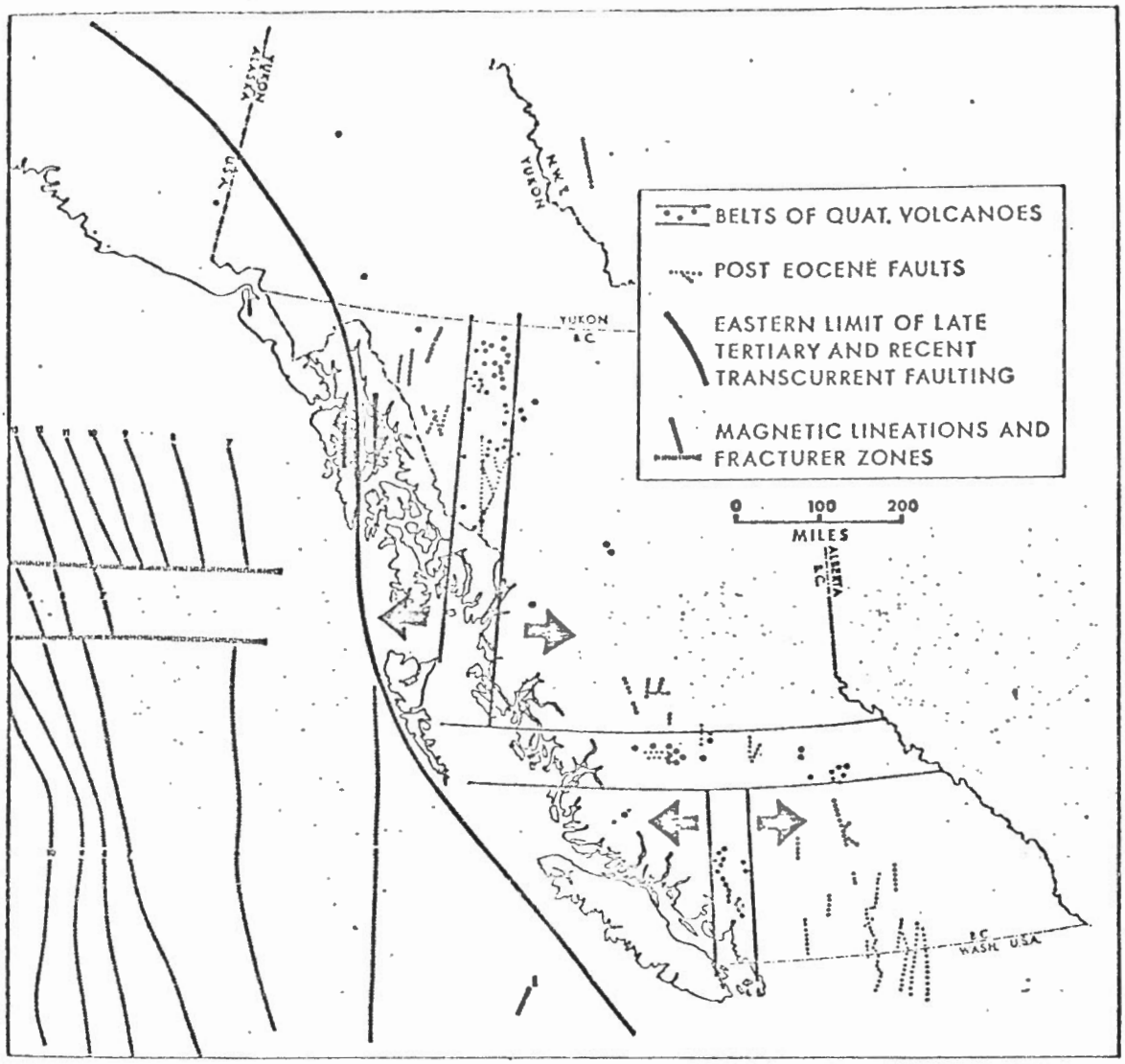

FIG. 8. Linear belts of Quaternary volcanoes in British Columbia and magnetic lineations and fracture zones in the Pacific (from Pitman and Hayes 1968). Arrows indicate present directions of inferred relative motion between adjacent segments of the Cordillera (E–W extension) and between the Cordillera and adjacent Pacific (right-lateral shear).

Figure 36: Hypothèse de SOUTHER
- SOUTHER Hypothesis

Figure 37 : RECONNAISSANCE M.T. LILLOUET

S.M.T. / M.T.S. STATION S.1

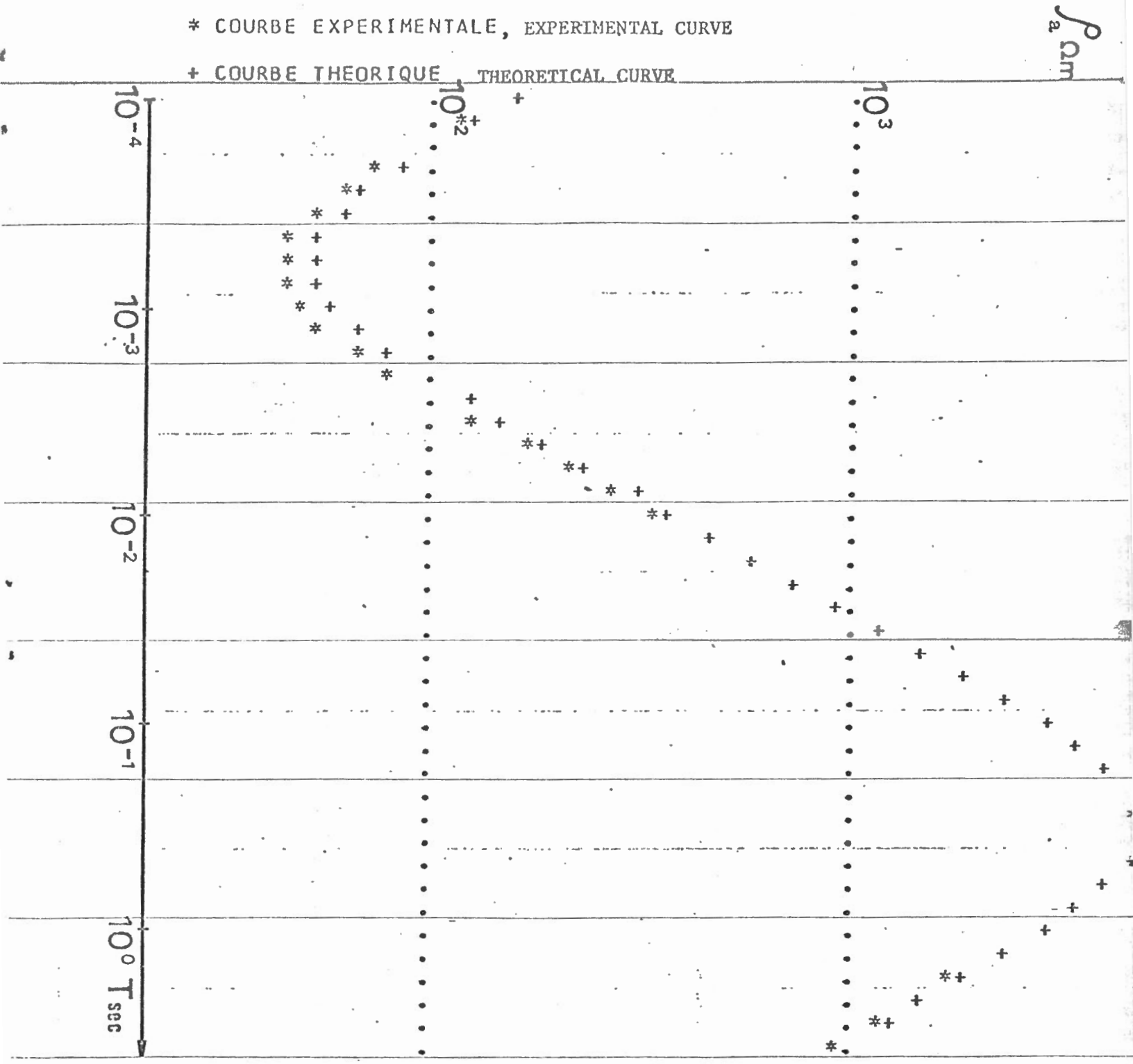

RO 1= 0.100000E 04 Ωm H 1= 0.450000E-01 km

RO 2= 0.250000E 01 H 2= 0.400000E-02

RO 3= 0.200000E 05 H 3= 0.200000E 02

Figure 38 : RECONNAISSANCE M.T. LILLOUET

S.M.T.
M.T.S. STATION S.2

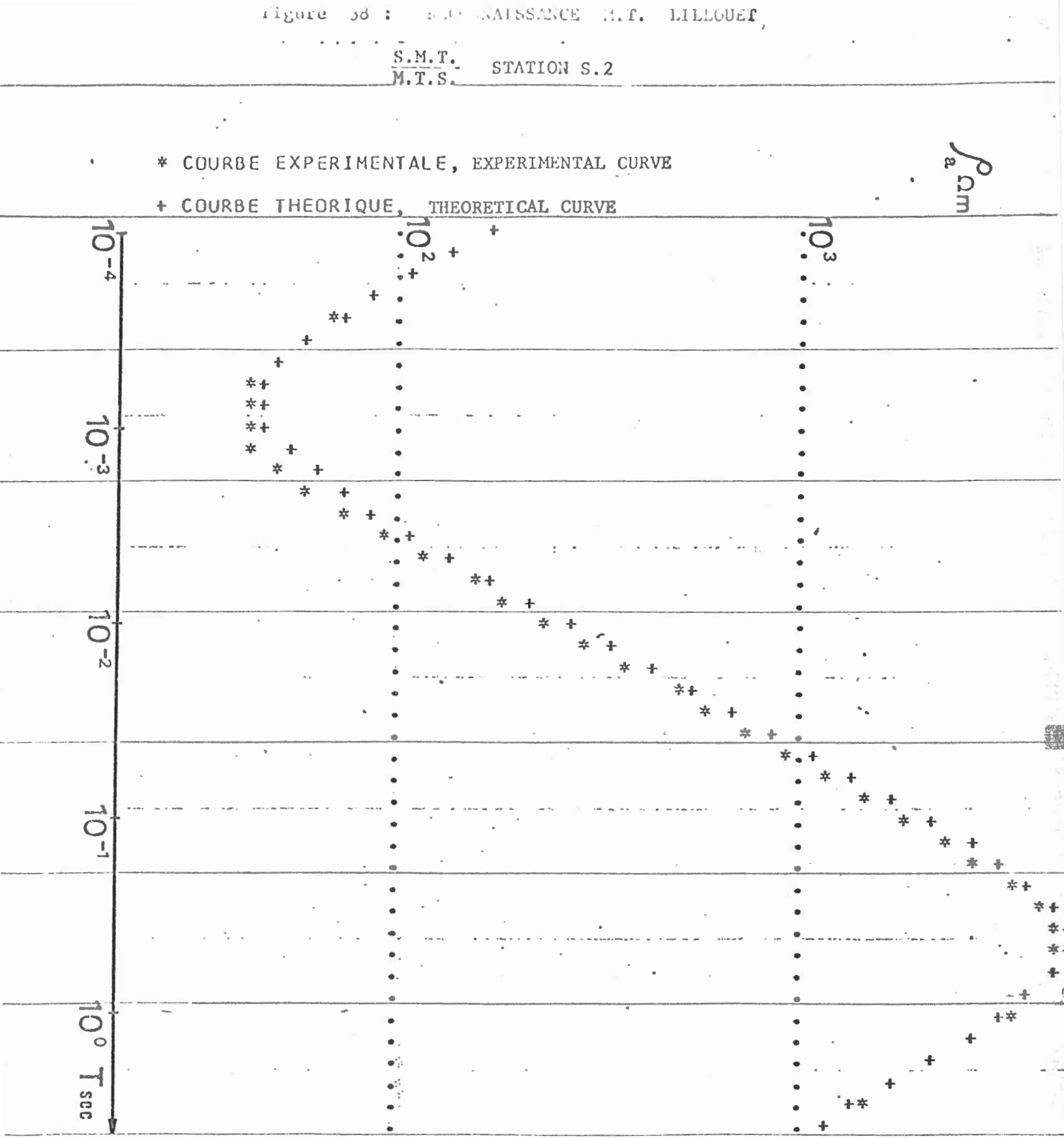

RO 1= 0.100000E 04 Ωm H 1= 0.450000E-01 km

RO 2= 0.250000E 01 H 2= 0.500000E-02

RO 3= 0.200000E 05 H 3= 0.210000E 02

STATION S.3 & S.4

* COURBE EXPERIMENTALE, EXPERIMENTAL CURVE

+ COURBE THEORIQUE; THEORETICAL CURVE

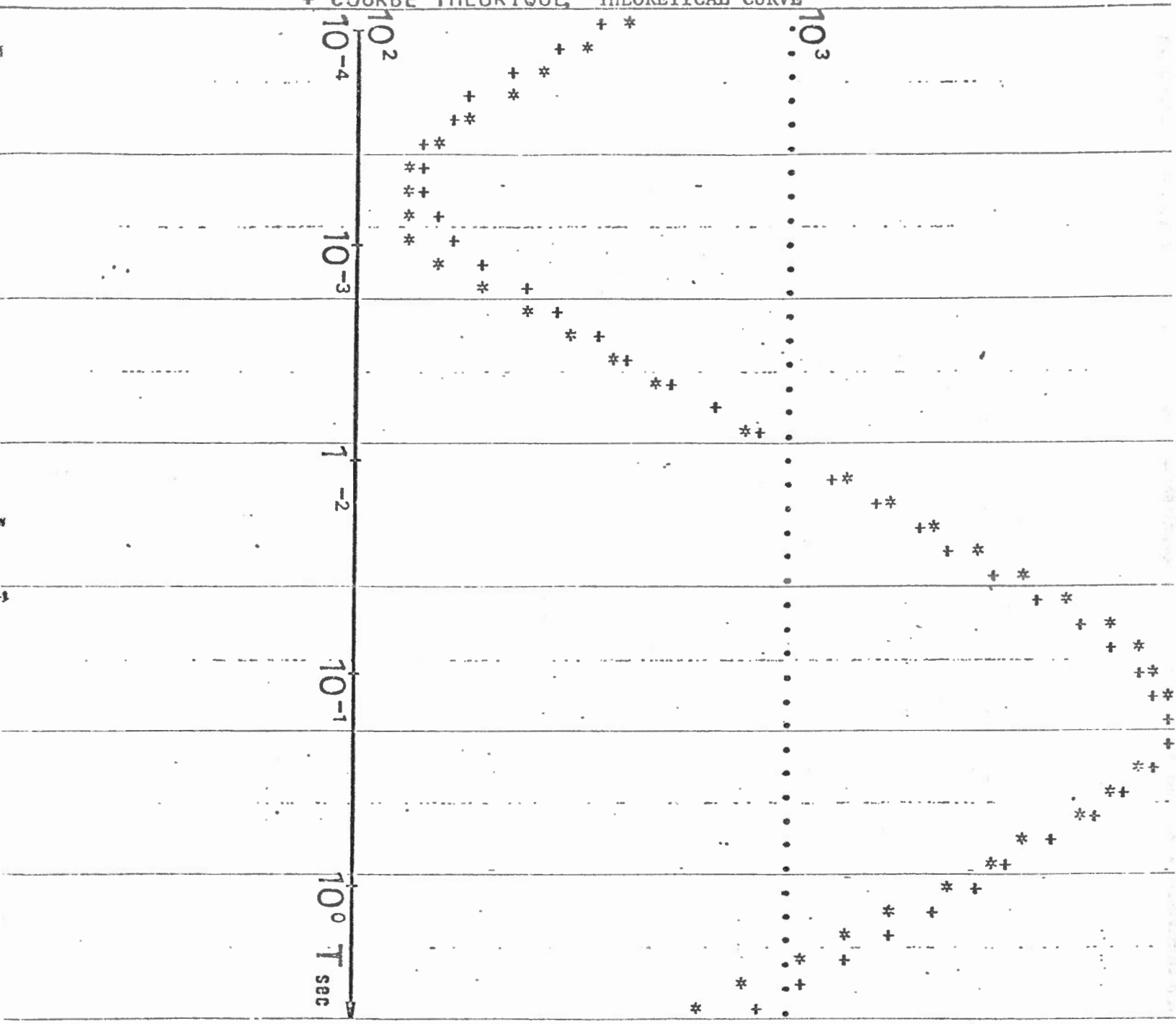

RO 1= 0.300000E 04Ωm H 1= 0.650000E-01 km

RO 2= 0.550000E 01 H 2= 0.500000E-02

RO 3= 0.200000E 05 H 3= 0.180000E 02

Figure 40 : RECONNAISSANCE M.T. LILLOUET

S.M.T. / M.T.S. STATION S.5

* COURBE EXPERIMENTALE, EXPERIMENTAL CURVE

\+ COURBE THEORIQUE, THEORETICAL CURVE

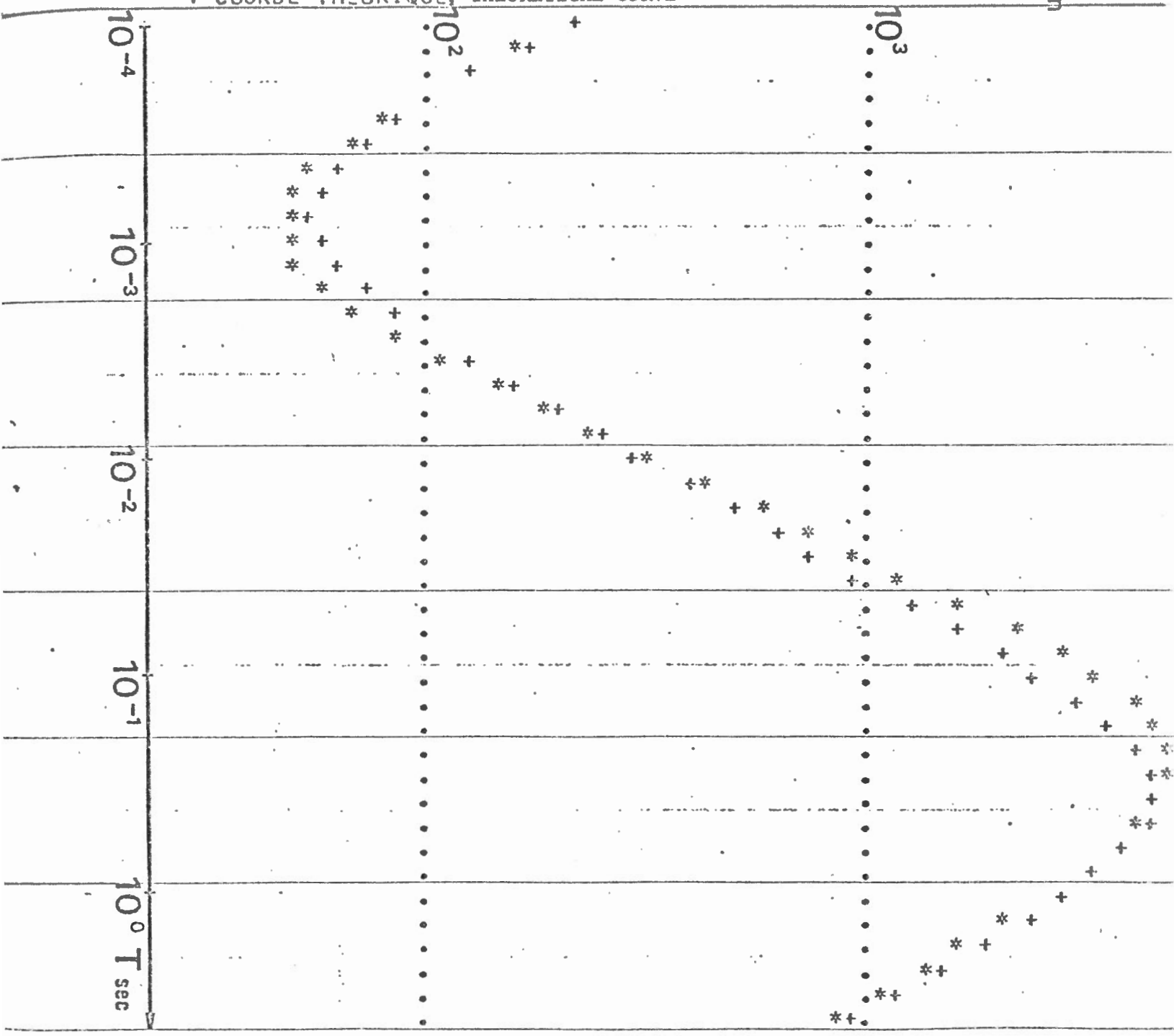

RO 1= 0.100000E 04 Ωm H 1= 0.500000E-01 km

RO 2= 0.270000E 01 H 2= 0.500000E-02

RO 3= 0.200000E 05 H 3= 0.190000E 02